Università degli Studi di Ferrara

Validation of a Monte Carlo method for the calibration of an airborne gamma-ray detector

Advisor Dr. Fabio Mantovani

Co-advisor Dr. Gerti Xhixha

Graduating Marica Baldoncini

Outline

- Airborne Gamma-Ray Spectroscopy (AGRS)
- Monte Carlo simulation strategy
- Comparison between Monte Carlo output and theoretical predictions
- Ground based calibration measurements with the AGRS_16L
- Airborne survey for AGRS_16L calibration at different altitudes
- Conclusions and perspectives

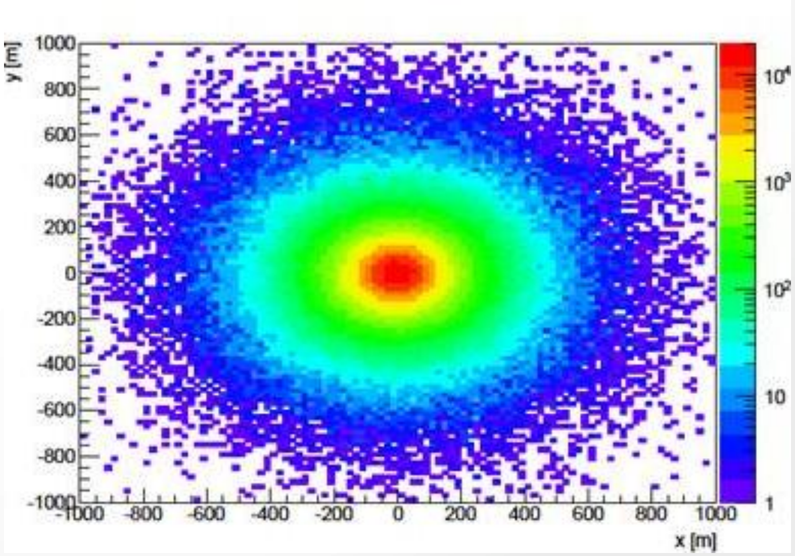

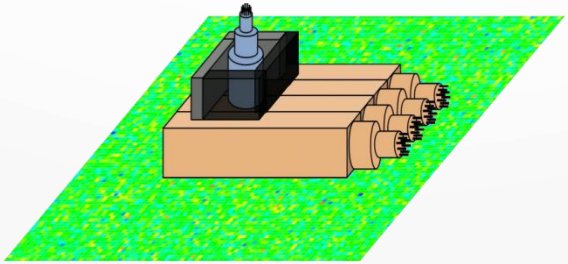

Radionuclides of terrestrial origin investigated with gamma-ray spectroscopy

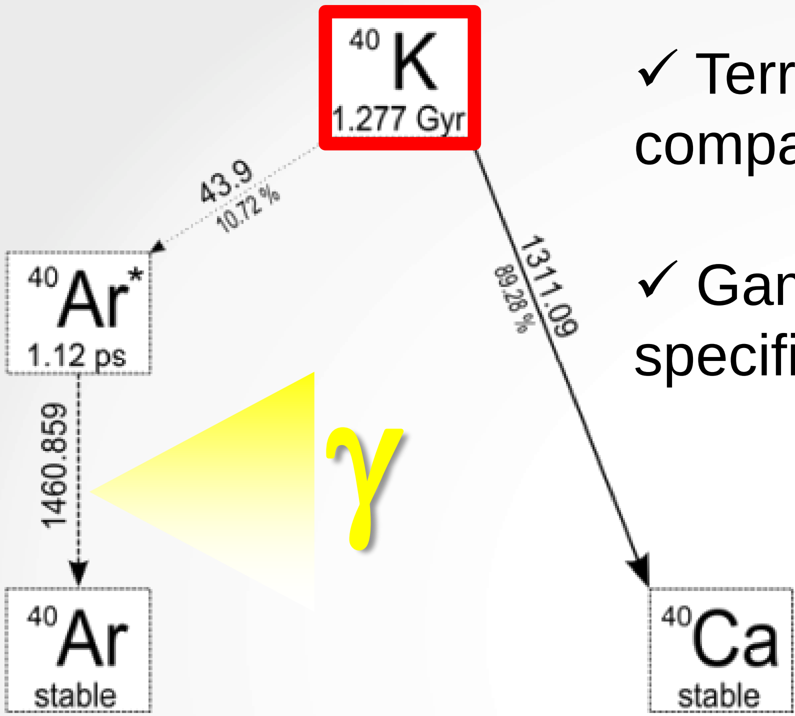

✓ Terrestrial radionuclides have half-lives comparable to Solar System age

✓ Gamma signal is a fingerprint of a specific decay

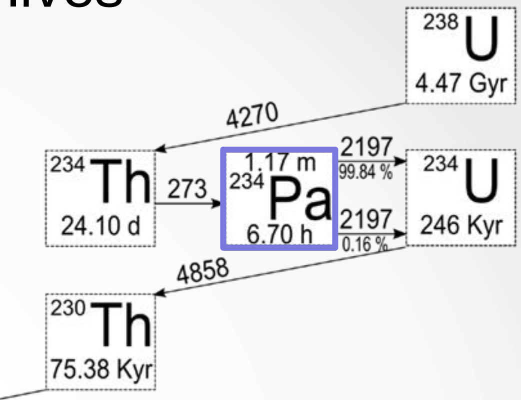

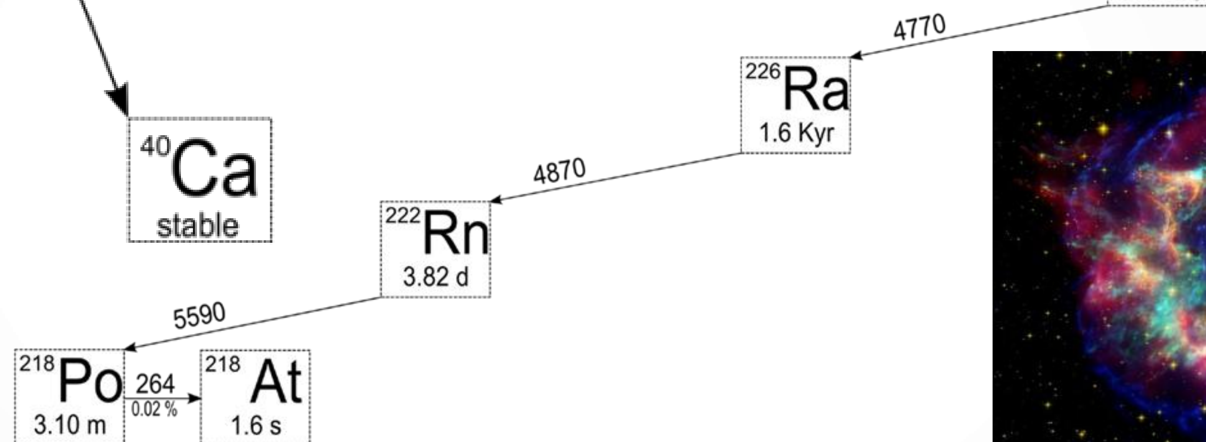

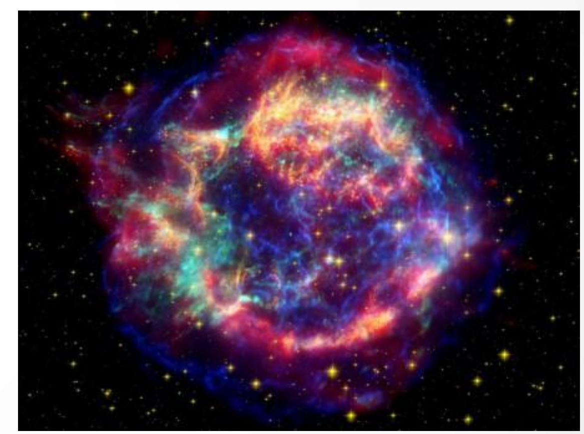

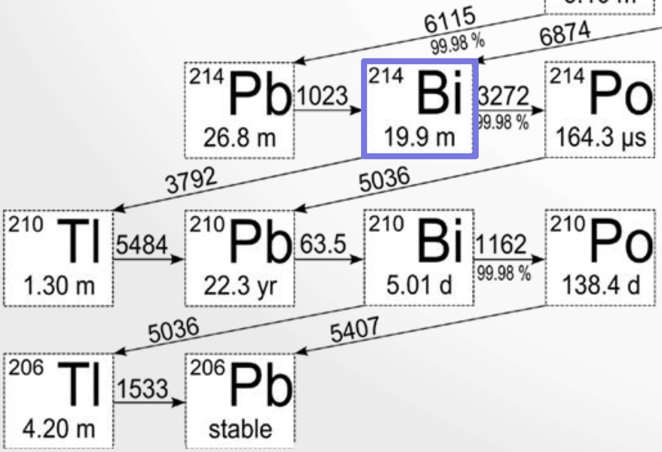

Radioisotope	Daughter	Energy (keV)	Half life	Typical abund.
^{40}K	/	1460	1.3 Gy	2%
^{238}U	^{234}Pa, ^{214}Bi	609, 1120, 1765	4.5 Gy	3 μg/g
^{232}Th	^{228}Ac, ^{208}Tl	911, 2614	14.1 Gy	10 μg/g

Airborne Gamma-Ray Spectroscopy (AGRS)

A typical spectrum acquired by AGRS_16L at 100 m (standard flight height) for 1s acquisition.

Total counts: ~ 600

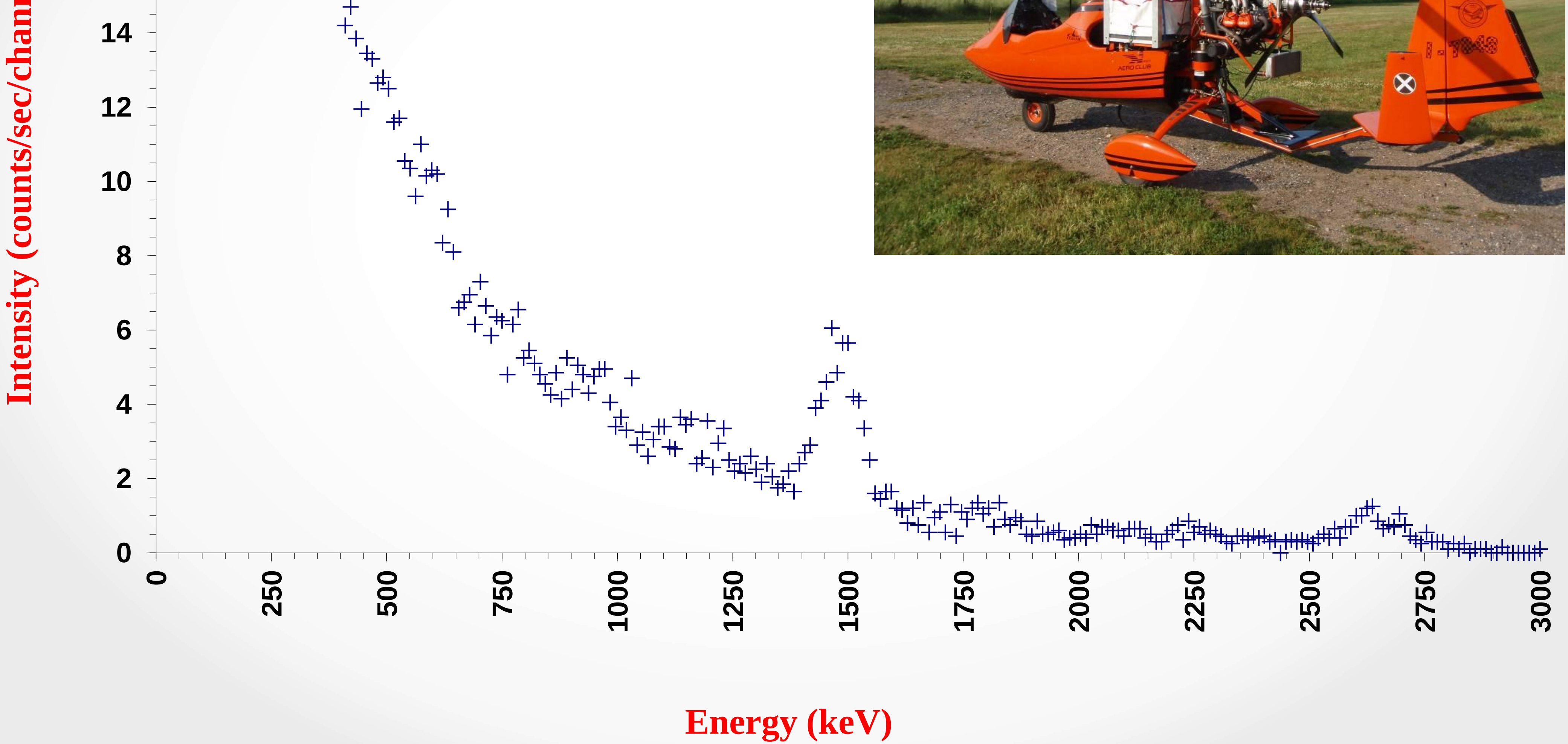

The Full Spectrum Analysis (FSA)

Total spectrum = individual radionuclide spectra + background spectrum

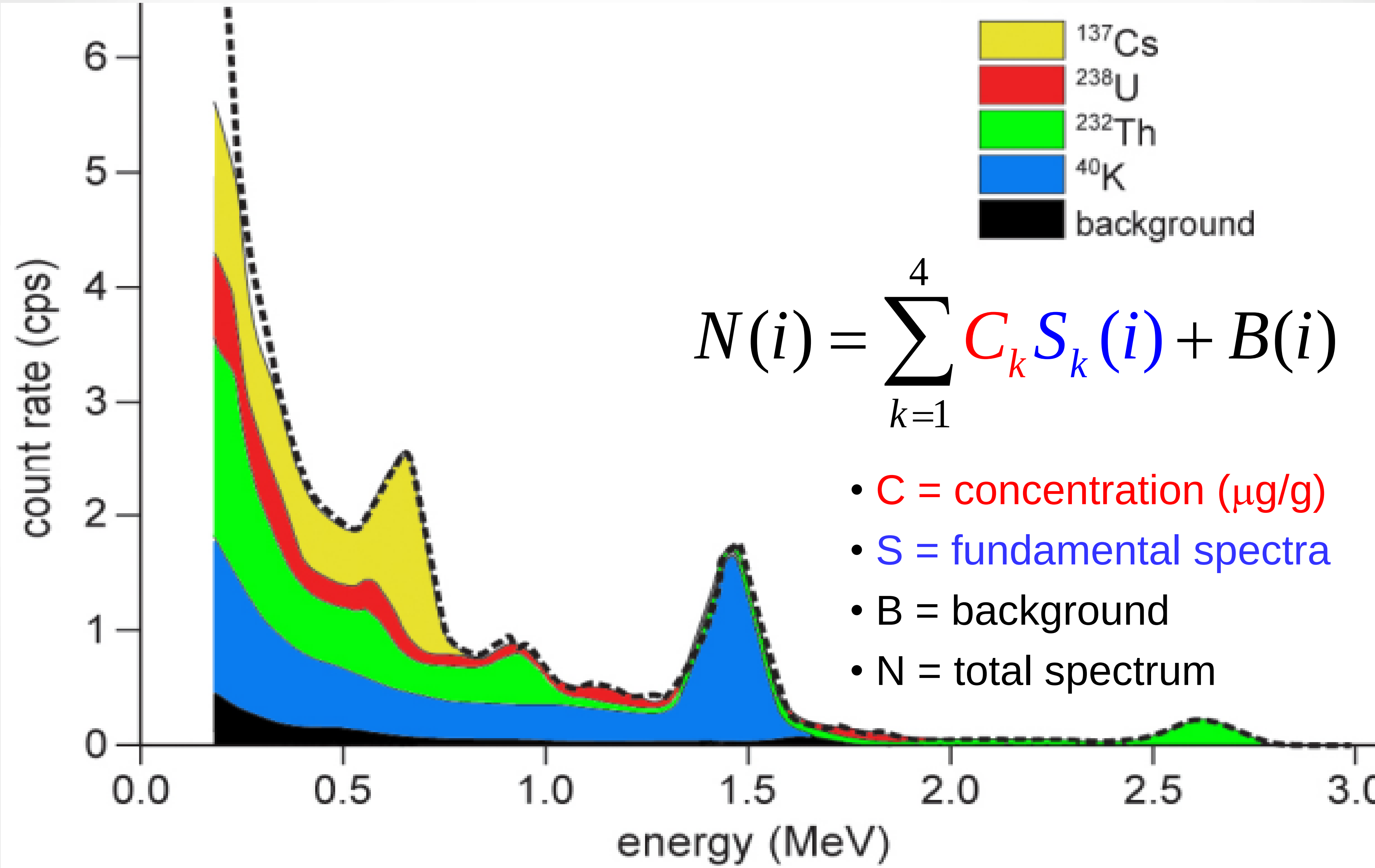

$$N(i) = \sum_{k=1}^{4} C_k S_k(i) + B(i)$$

- C = concentration (μg/g)
- S = fundamental spectra
- B = background
- N = total spectrum

Scientific and technological motivations

Noise from atmospheric ‘invisible’ radon?

Signal correction for the height?

Attenuation due to vegetation?

Monte Carlo simulation is a suitable strategy!

Signal variation due to morphology?

Sensitivity to hot spots?

Effects due to soil density and chemical composition?

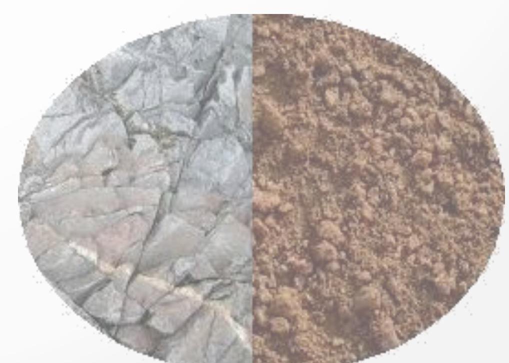

Direct simulation: impossible!

A direct simulation of the source-detector geometry would take a too much long computational time

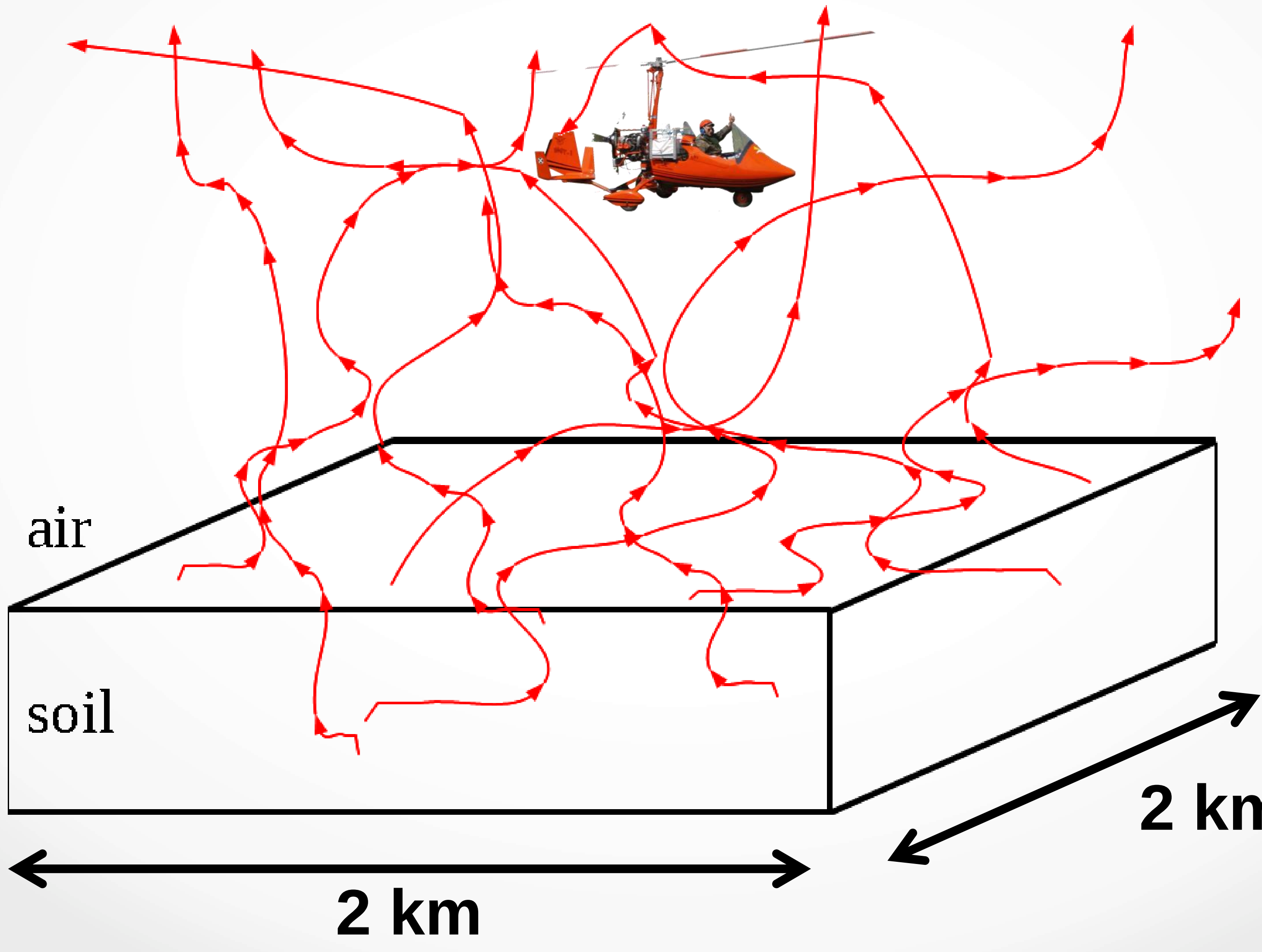

Monte Carlo simulation algorithms

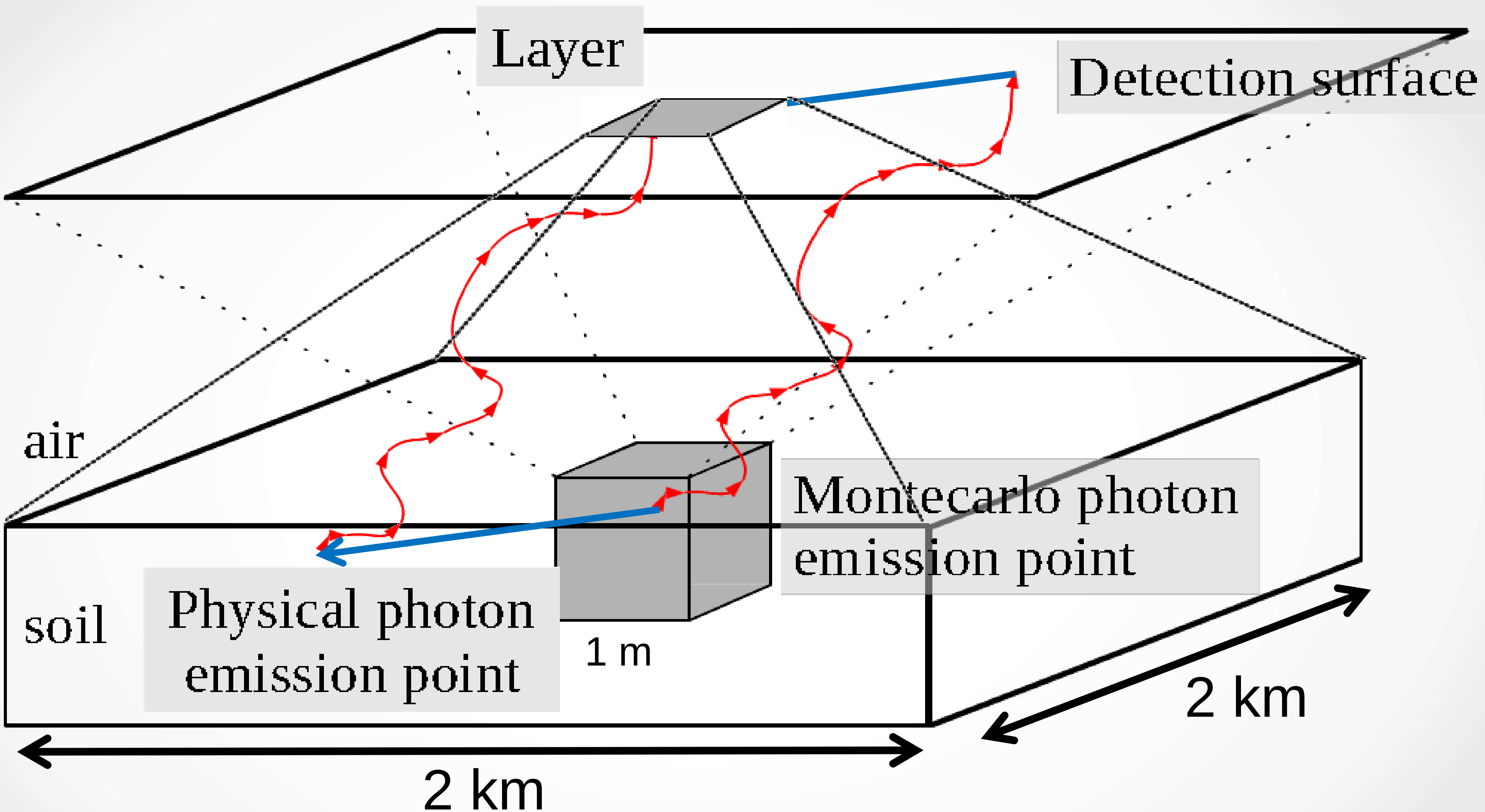

A shift of photon arrival position is equivalent to a shift of photon emission point, without changing photon track.

Effects of the geometrical transformation

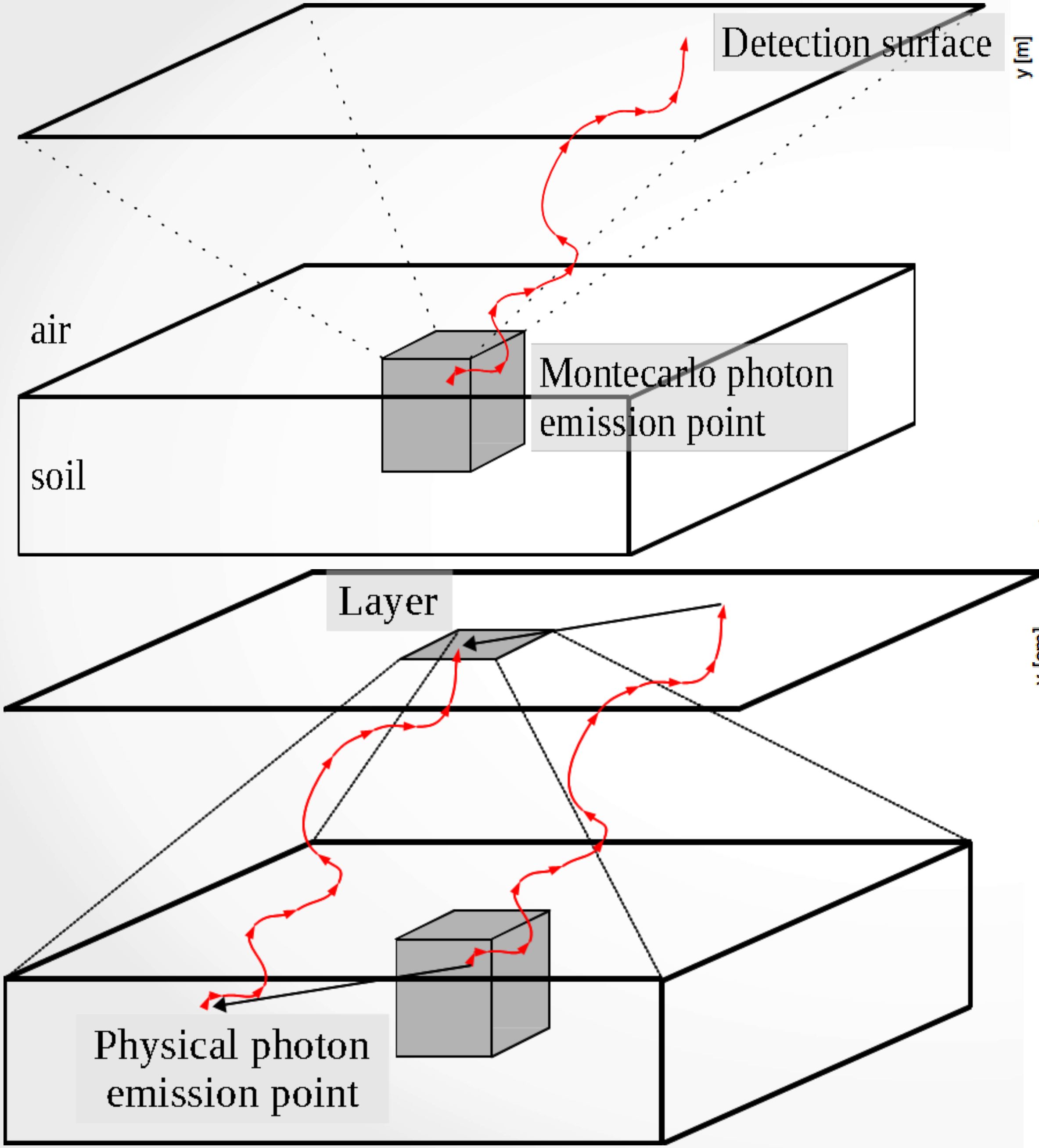

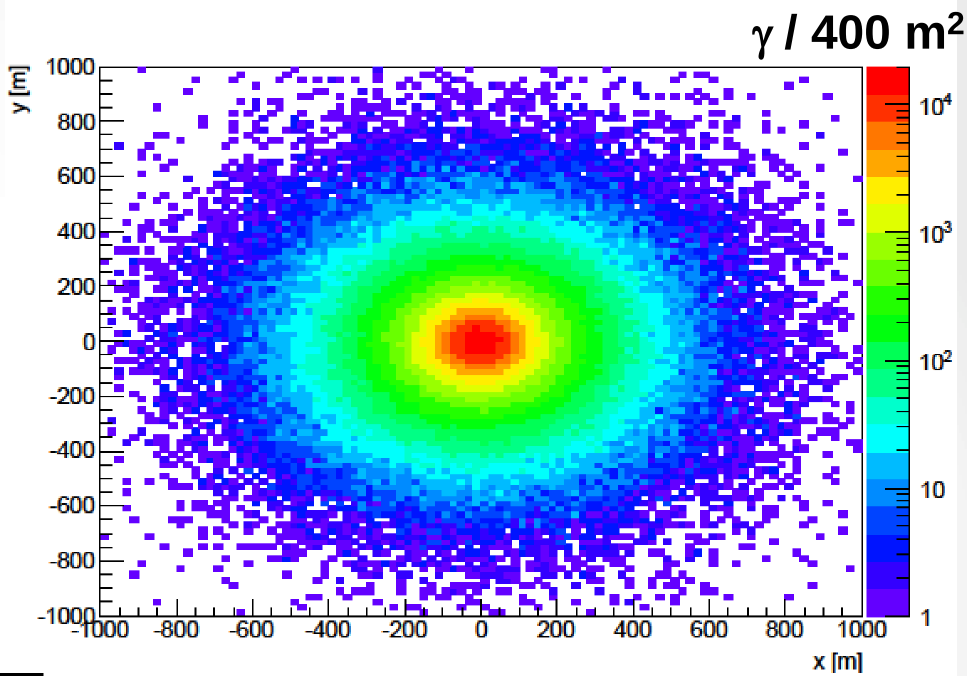

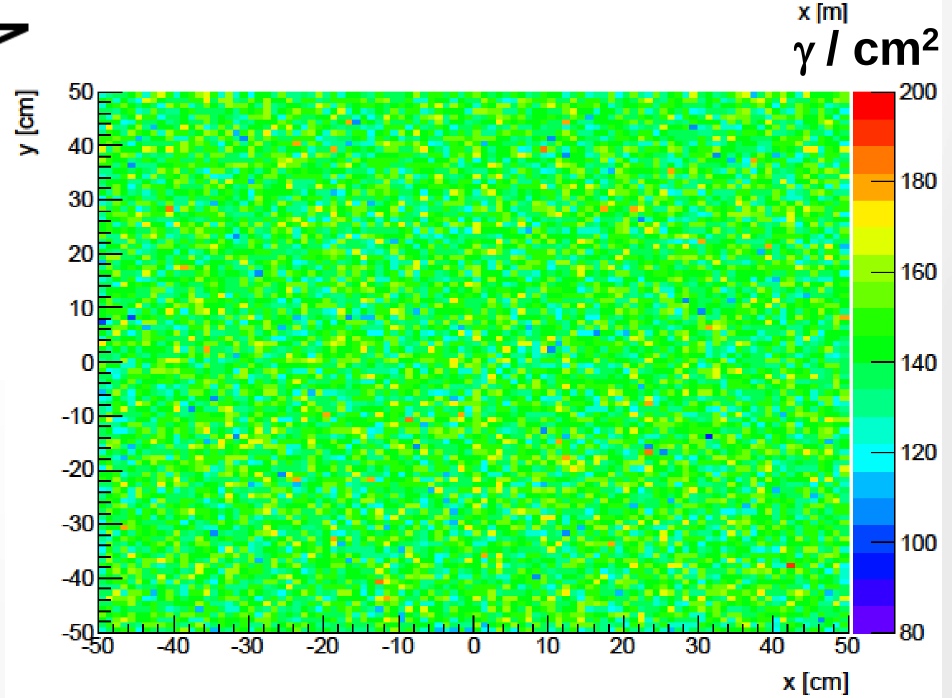

^{40}K photopeak flux from a point source: Monte Carlo Vs theory

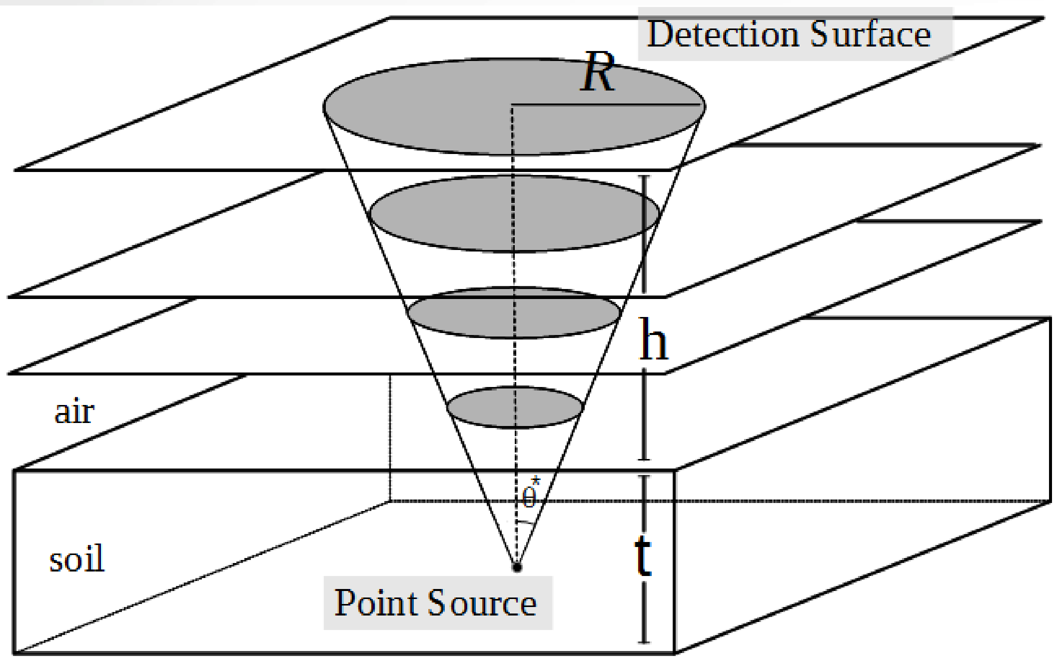

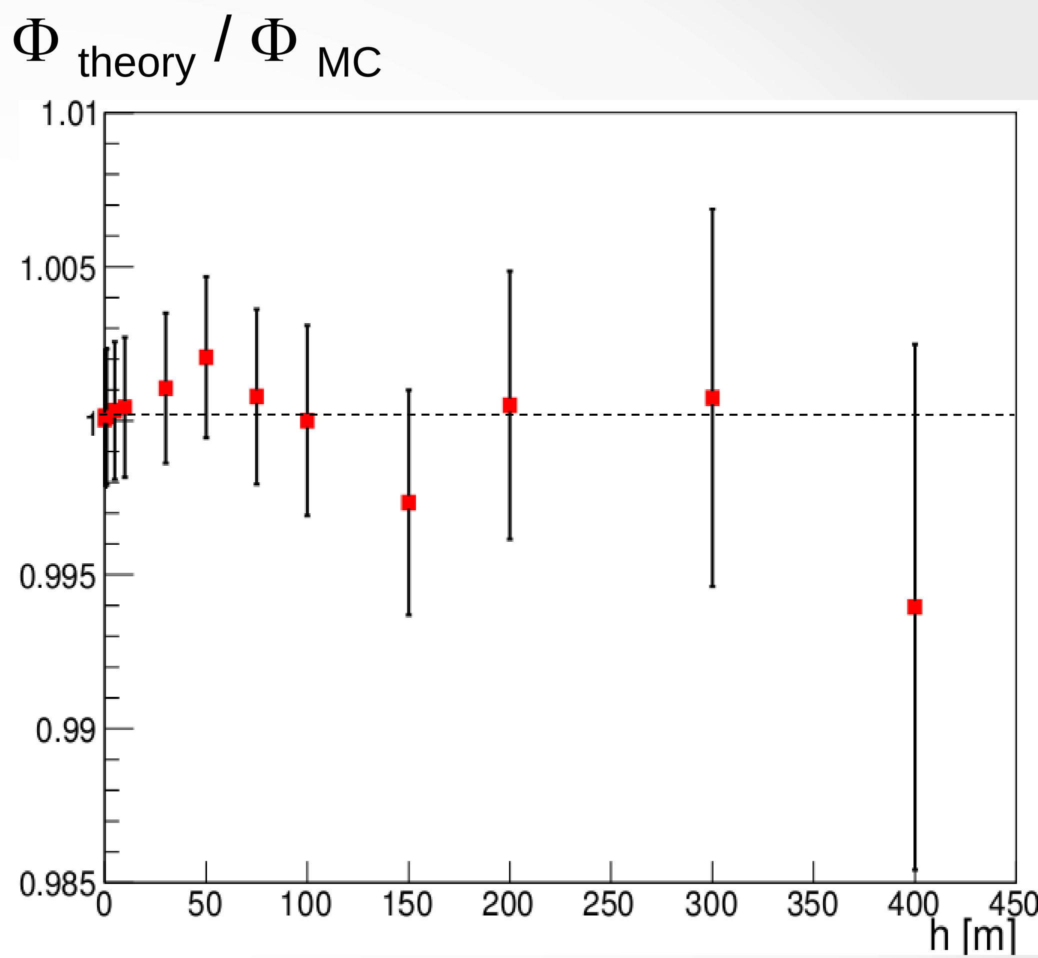

$$\Phi(h) = \frac{N_h}{\pi R^2}$$

N_h = number of photopeak counts at height h

πR^2 = area of the circular surface

^{40}K photopeak counts from a diffuse source: Monte Carlo Vs theory

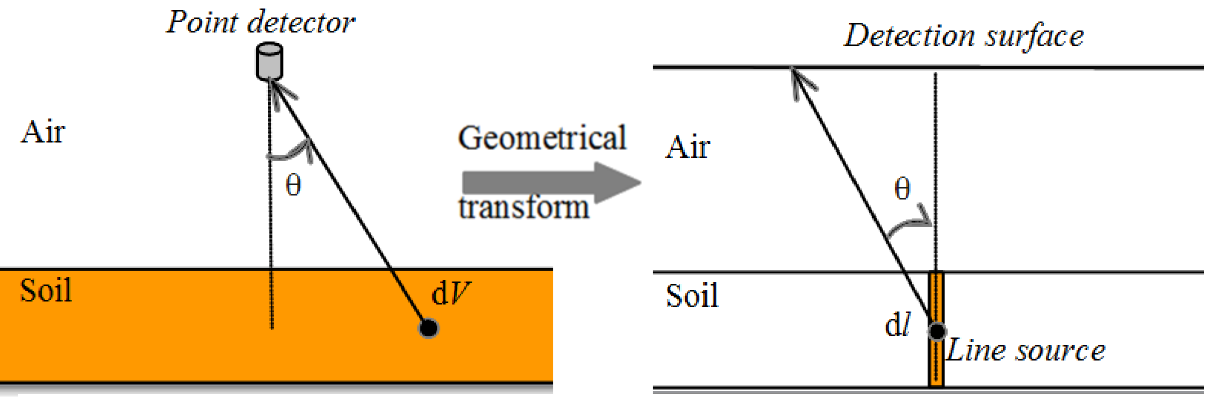

$$\text{Theory: } \psi(h) = \frac{N(h)}{N(0)} = \frac{E_3(\mu h)}{E_3(0)}$$

$$= \frac{\int_0^{\pi/2} d\theta \sin\theta \cos\theta \; e^{-\frac{\mu h}{\cos\theta}}}{\int_0^{\pi/2} d\theta \sin\theta \cos\theta}$$

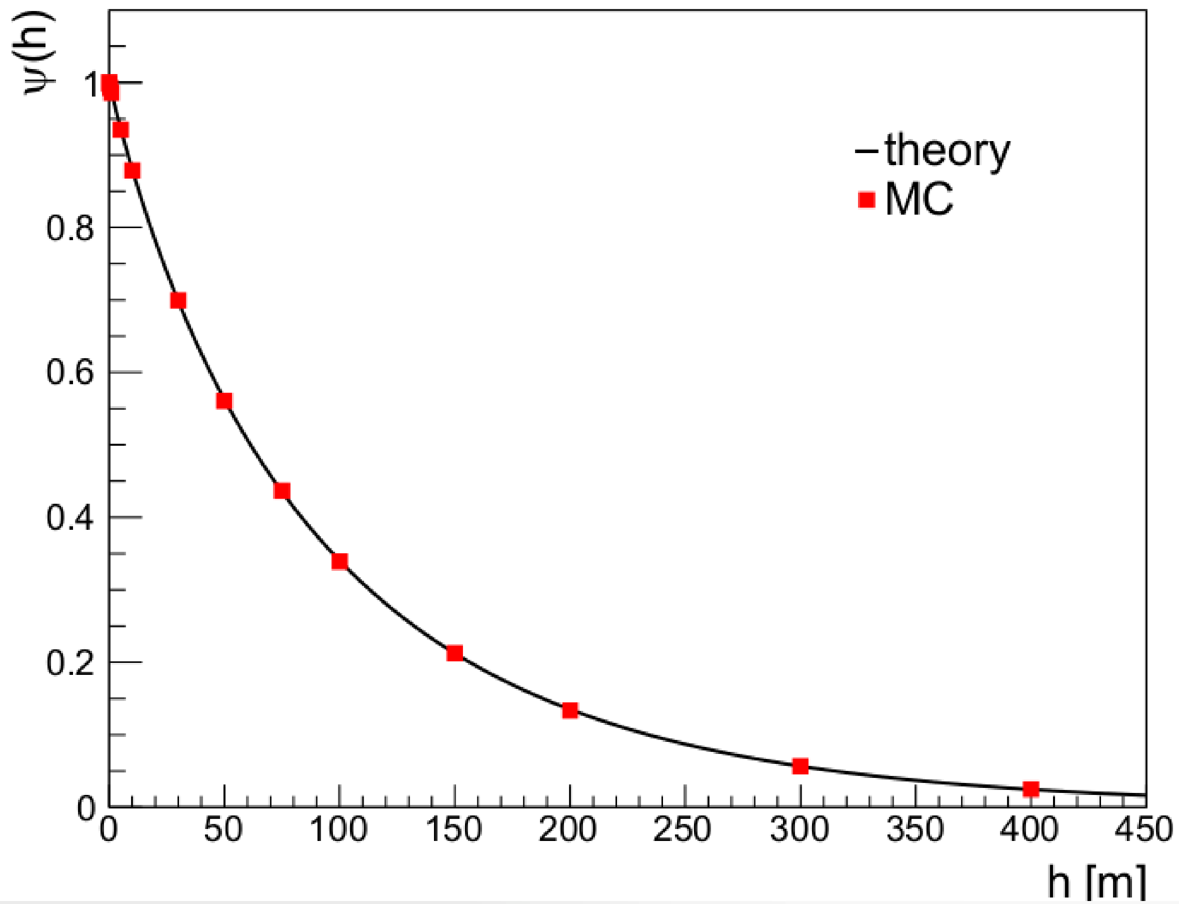

✓ Theory based on analytically unsolvable exponential integrals

✓ Theoretical predictions depend on empirical parameters (linear attenuation coefficient μ)

Excellent agreement with different inputs

AGRS_16L design and features

AGRS_16L		MC
4 NaI(Tl) detector	4 Lit. (102 mm x 102 mm x 406 mm)	✓
4 steel housings	Thick.=1 mm, Top=11mm, Bottom=4.75mm	✓
4 PMT	Radius=45mm, Length=146mm	✓
PVC box	Thickness=10mm	✓
1 NaI(Tl) detector	1 Lit. (102 mm x 102 mm x 102 mm)	✓
Channels	2048 (1024, 512, 256)	✓
Real-time feedback	notebook (smartphone & tablet)	
Power supply	12V battery	✓
Weight (total)	~ 115 kg	
Output	List mode events	
Auxiliary sensors	GPS antenna, P & T Sensors	

The model detector has ideal energy resolution

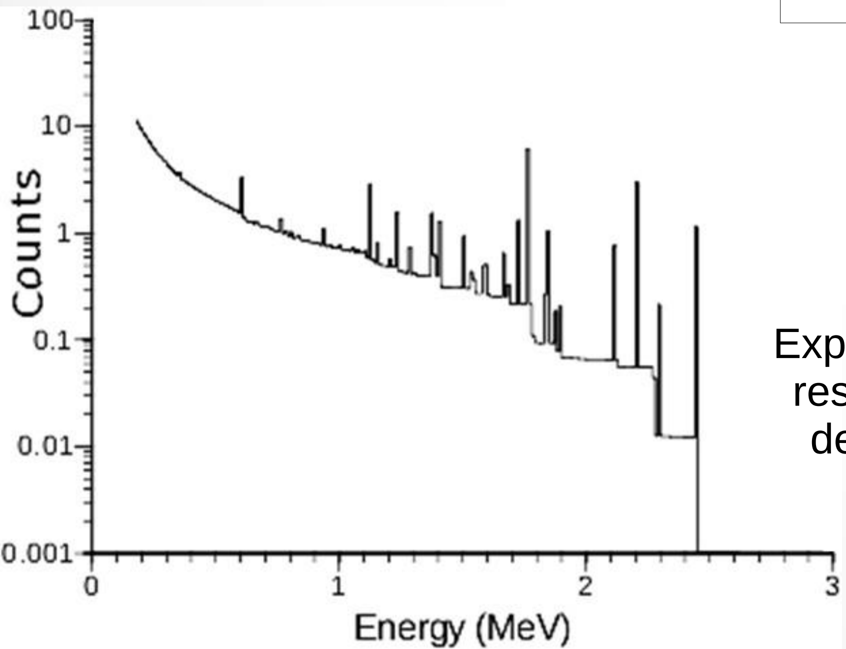

Experimental energy resolution for each detector channel

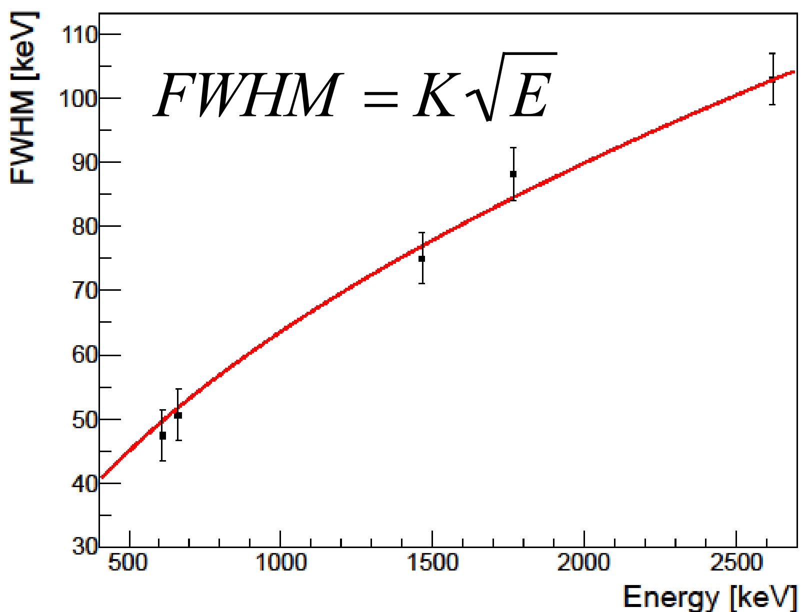

Ground based calibration spectra

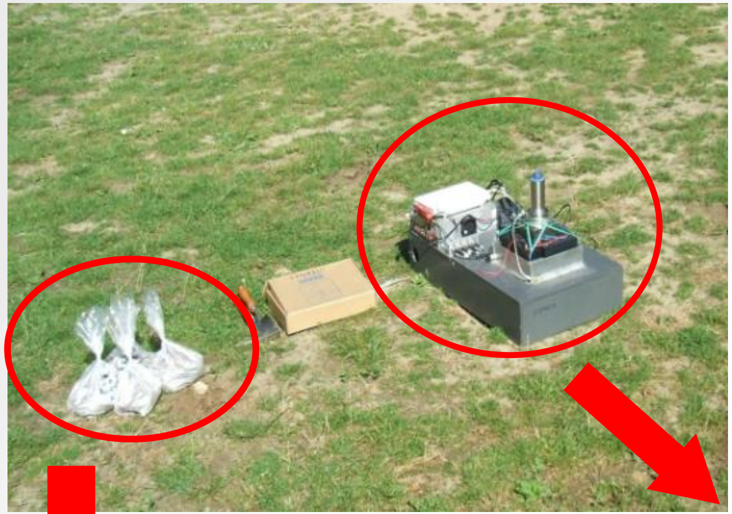

$$N = C \cdot FS$$

Experimental Fundamental Spectra (EFS)

Monte Carlo Fundamental Spectra (MCFS)

High-Purity Germanium (HPGe)

C = concentration

Monte Carlo and algorithm processes

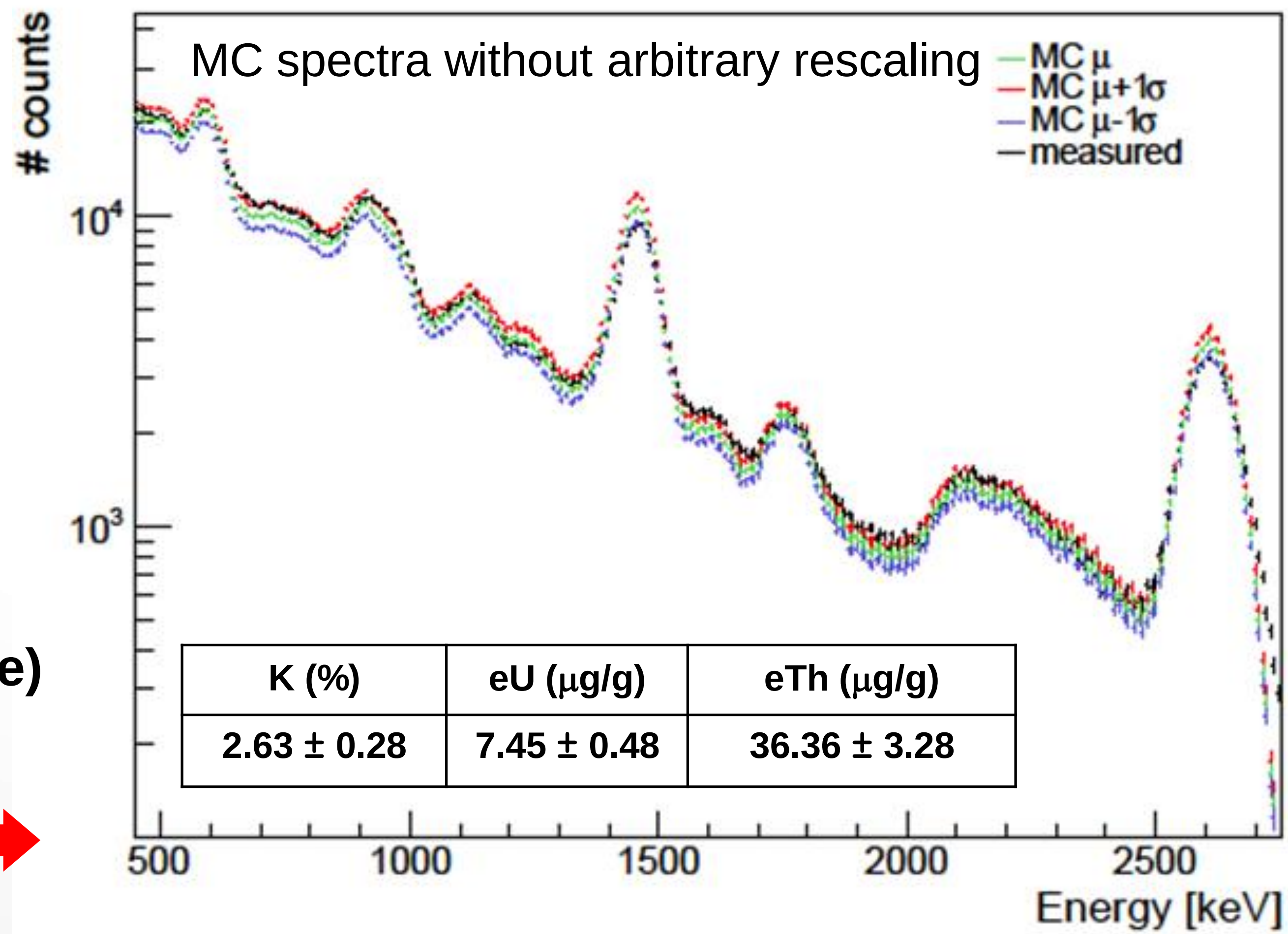

K (%)	eU (μg/g)	eTh (μg/g)
2.63 ± 0.28	7.45 ± 0.48	36.36 ± 3.28

Experimental Fundamental Spectra (EFS) and Monte Carlo Fundamental Spectra (MCFS)

EFS

χ^2

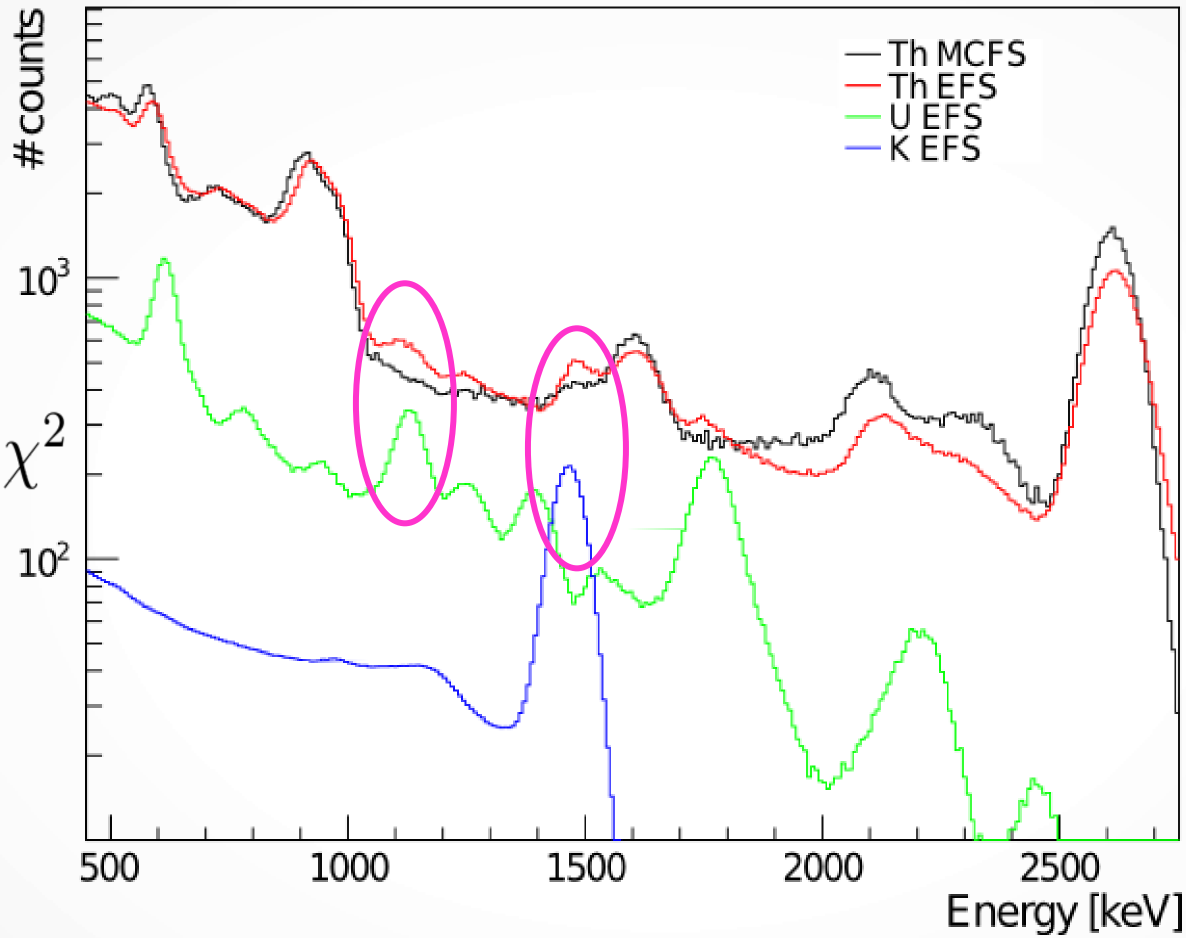

MCFS

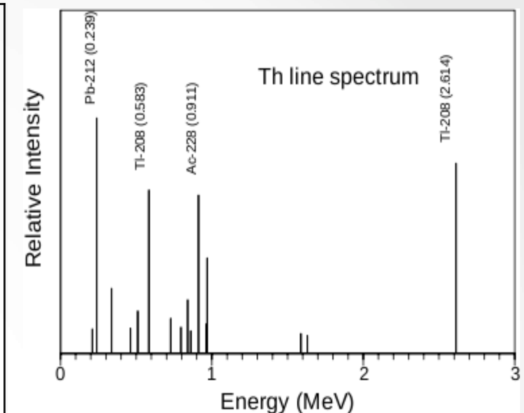

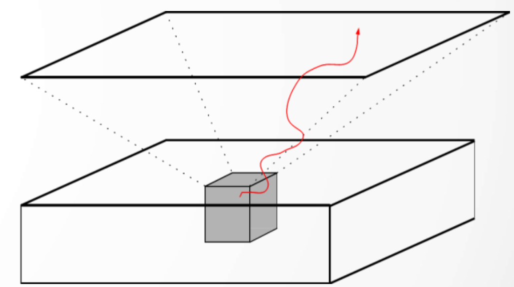

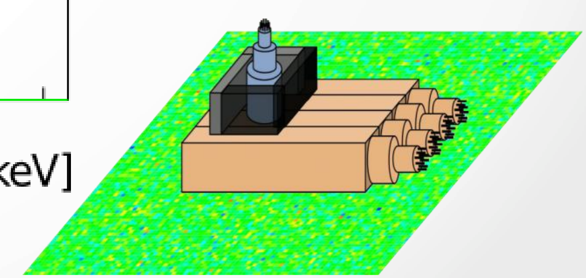

EFS show **residual interferences** between isotopes in the spectral shape

The χ^2 minimization process does not account for physical constraints

Each MCFS (K, U, Th) is determined independentely on the others

Changing soil density and composition

Same density (1.6 g/cm^3) and different composition

Carbonate (Z_{eff} = 10.5) and standard soil (Z_{eff} = 8.7)

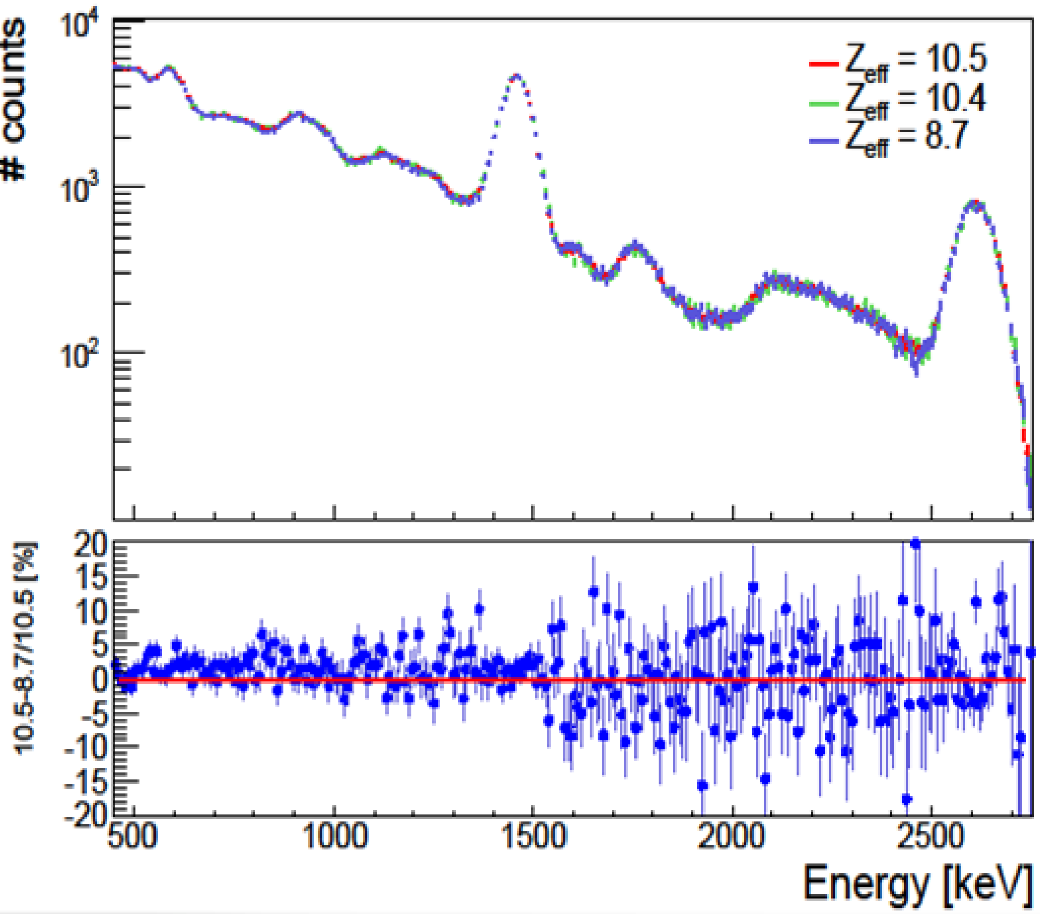

Same composition (Z_{eff} = 10.4) and different density

Typical soil density range: 1 ÷ 2 g/cm^3

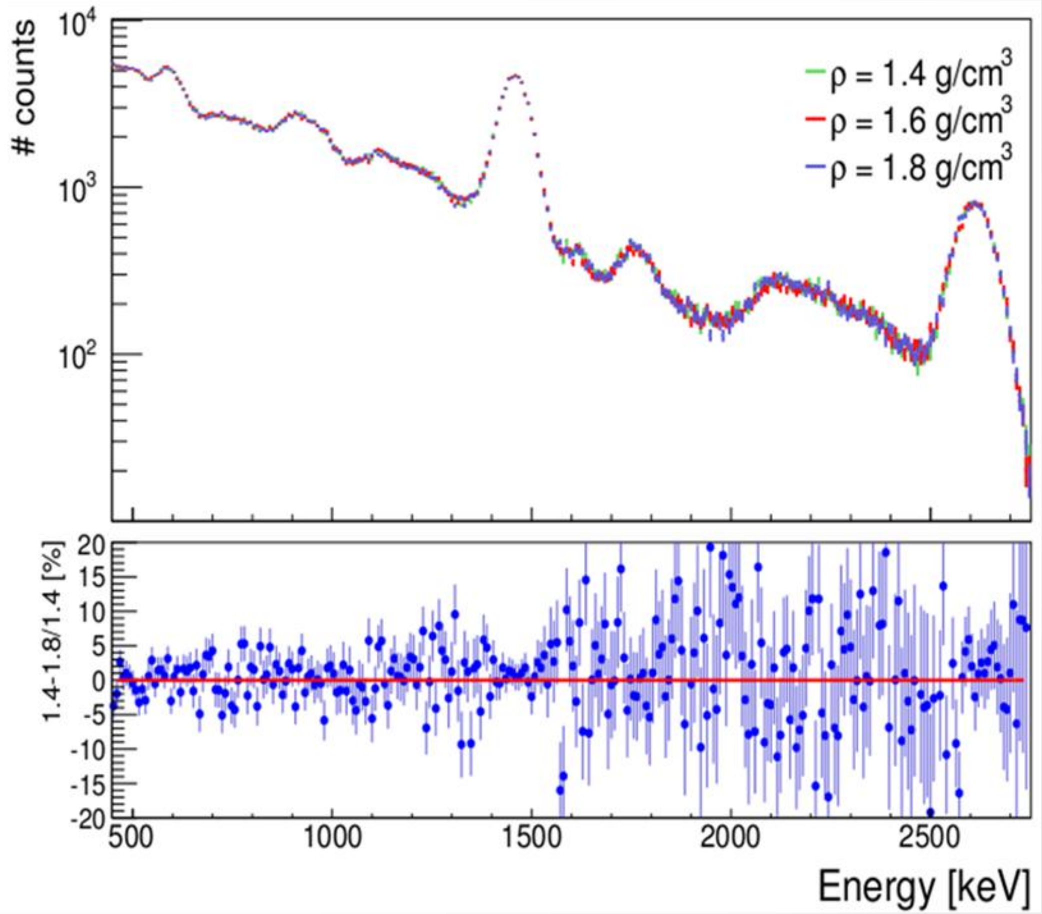

Mean residual less than 1% and no evident trends in the energy range

Overall effect on entire spectra smaller than abundances variability

Changing source-detector geometry

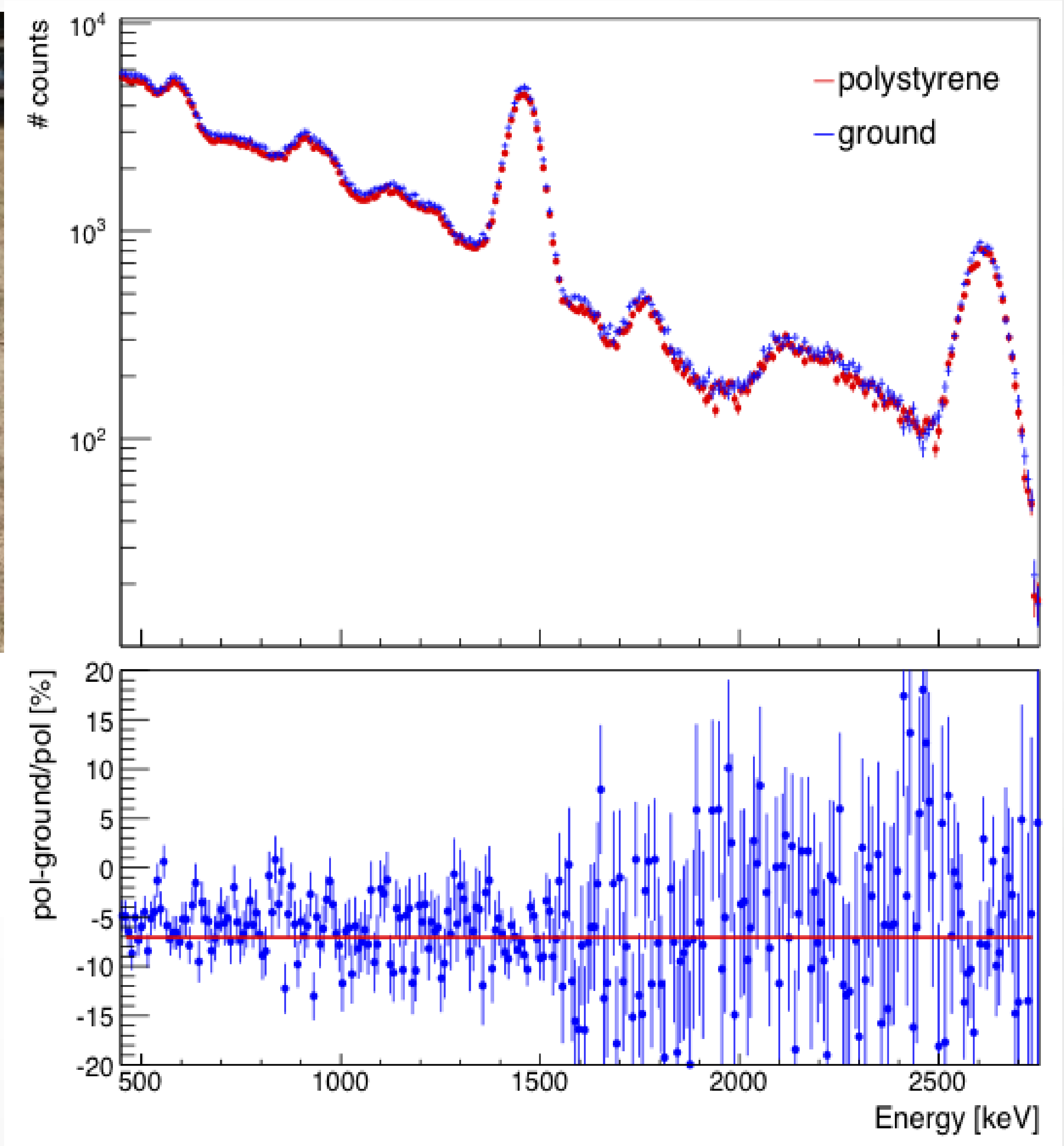

A 5 cm thick polystyrene layer produces a 7% mean attenuation with no evident distortion in the spectral shape

Taking off: ‘calibration’ on the fly...

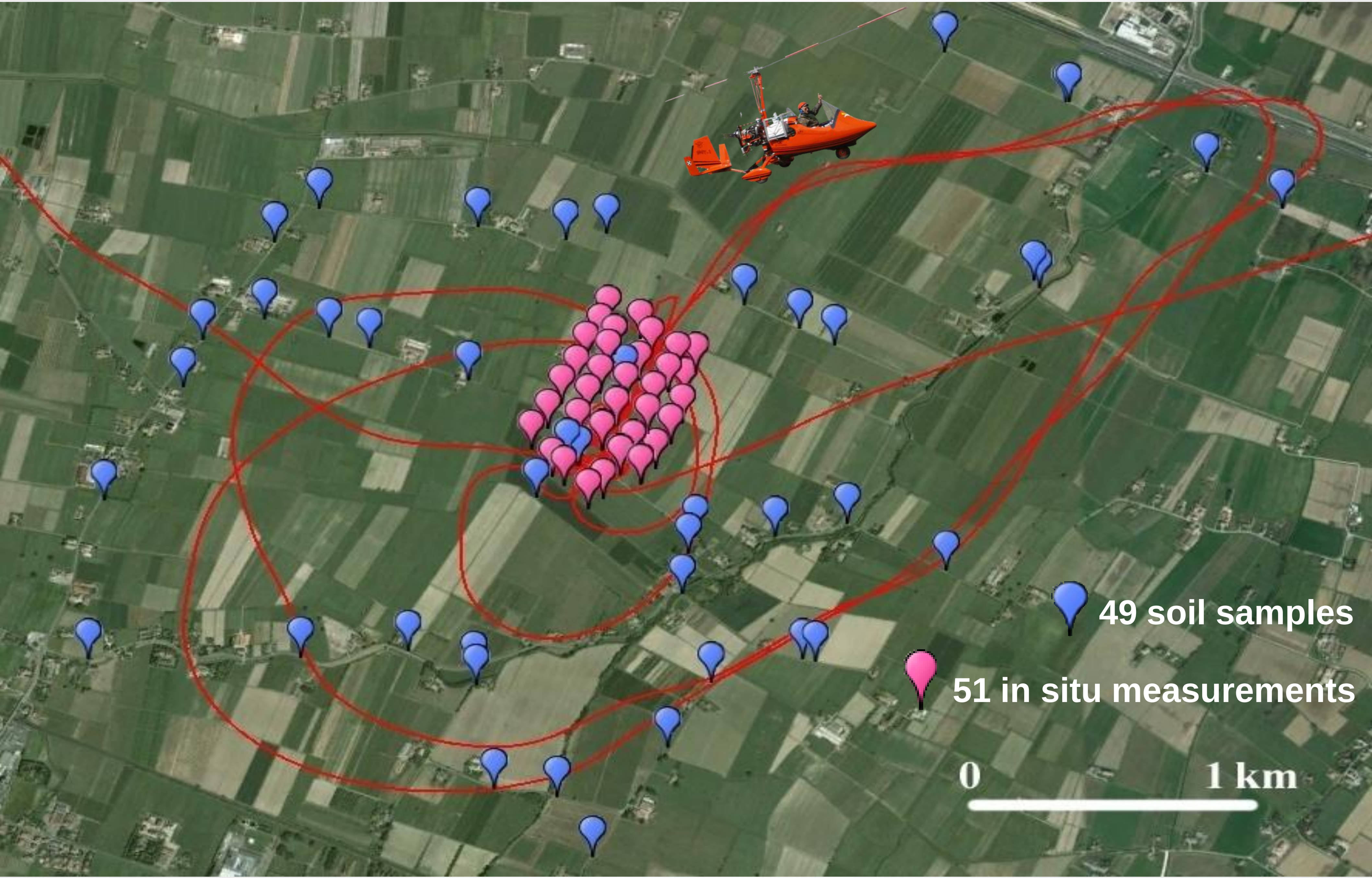

^{40}K photopeak at different altitudes: theory, MC and experiment

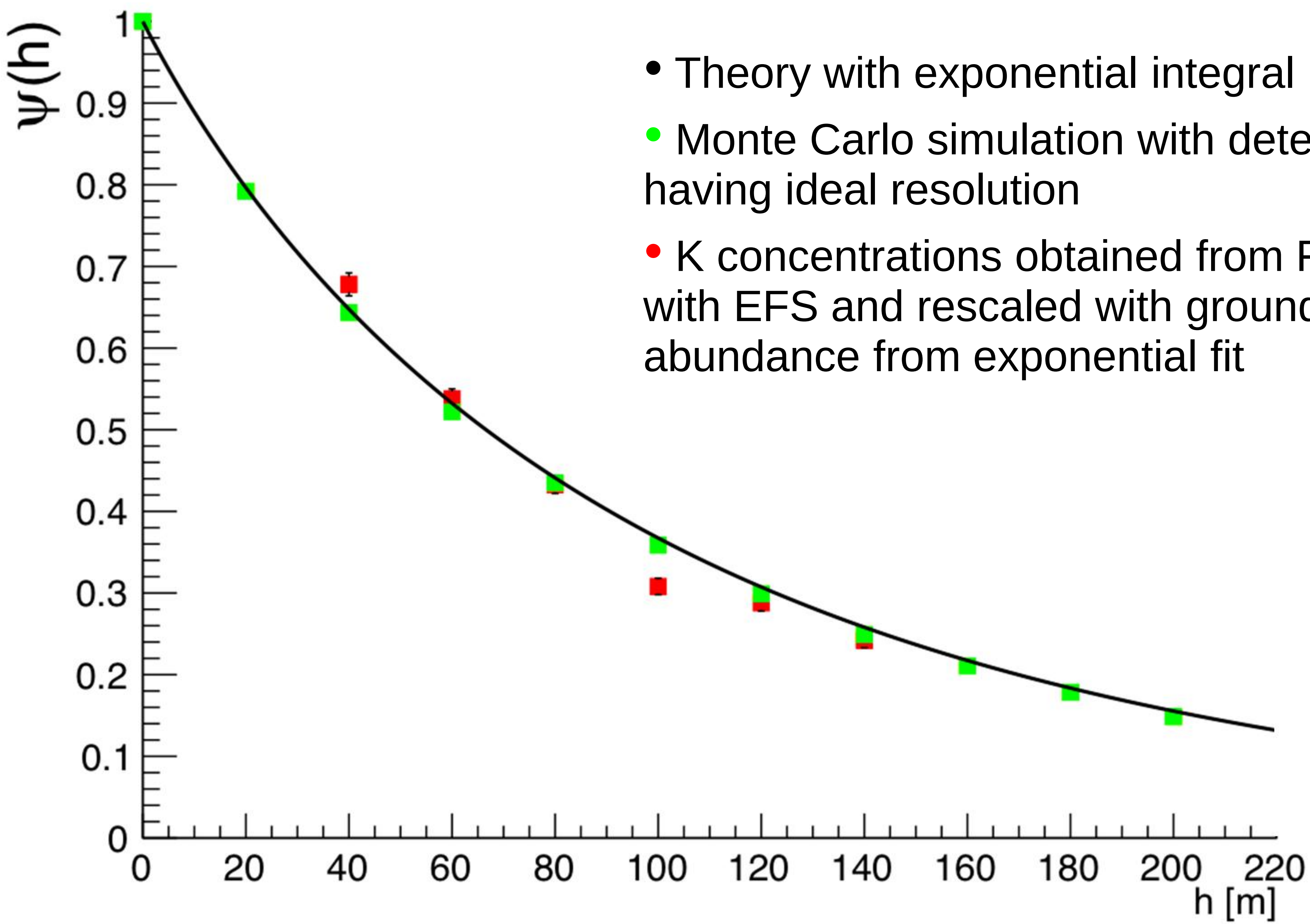

FSA of airborne survey with MCFS

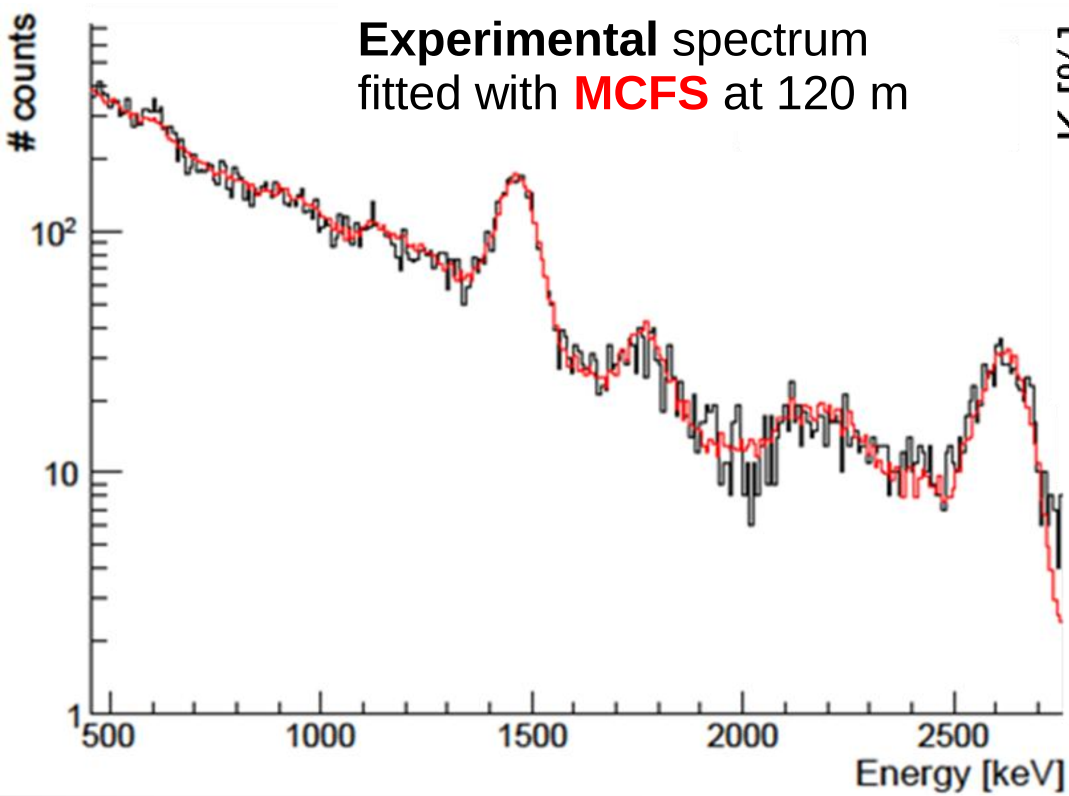

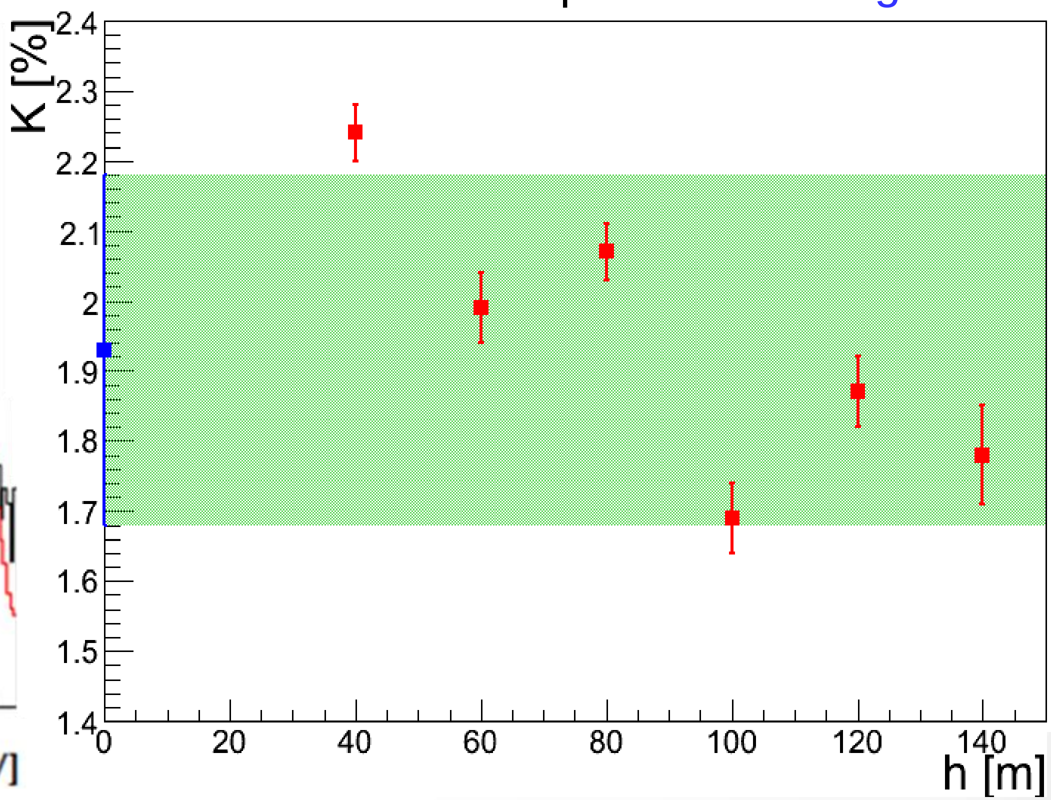

	K [%]	eU [μg/g]	eTh [μg/g]	χ^2
Ground	1.93 ± 0.25	2.35 ± 0.50	9.32 ± 1.09	/
EFS	2.05 ± 0.08	3.39 ± 0.19	10.47 ± 0.37	1.73
MCFS	1.69 ± 0.05	3.28 ± 0.20	9.37 ± 0.35	1.42

Abundances obtained at 100 m

Conclusions

- MC algorithms based on geometrical transformation have been developed to optimize the simulation of gamma-ray fluxes originating from infinite diffuse sources, solving the problem of direct simulation

- The MC outputs are rigorously compared with theoretical and analytical predictions under restricted physical constraints, obtaining always excellent agreement

- Ground based measurements have been well reconstructed without any rescaling. The MCFS do not suffer of residual correlations as EFS do

- Soil density and chemical composition are less critical parameters with respect to natural abundances variability

- Good agreement between airborne and fit spectra obtained using MCFS

- The FSA of airborne spectra with MCFS provides abundances in agreement at 1σ level with ground measurements.

Future perspectives

Radon noise is a challenge to measure, but hopefully we can simulate it.

Model a layer of vegetation/snow and compare with attenuation coefficient reported in literature

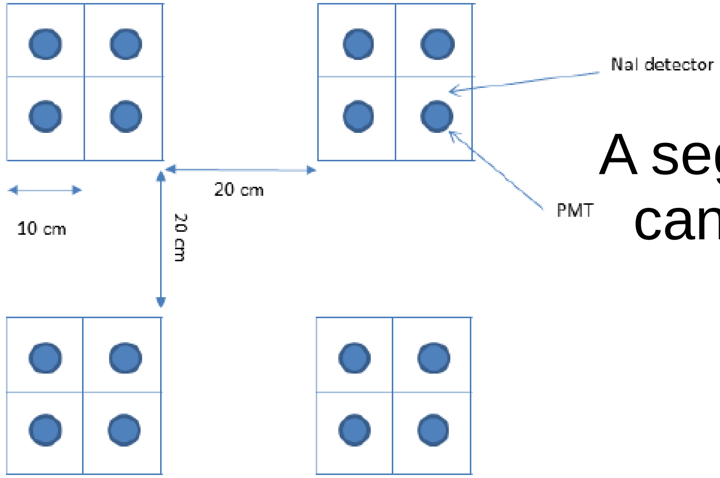

A segmented detector can give directional information, let’s test it!

What is the AGRS_16L sensitivity to “hot spots”? Simulation and new measurements are expected…

Thank you

Back-up slides

MCFS at different altitudes: K

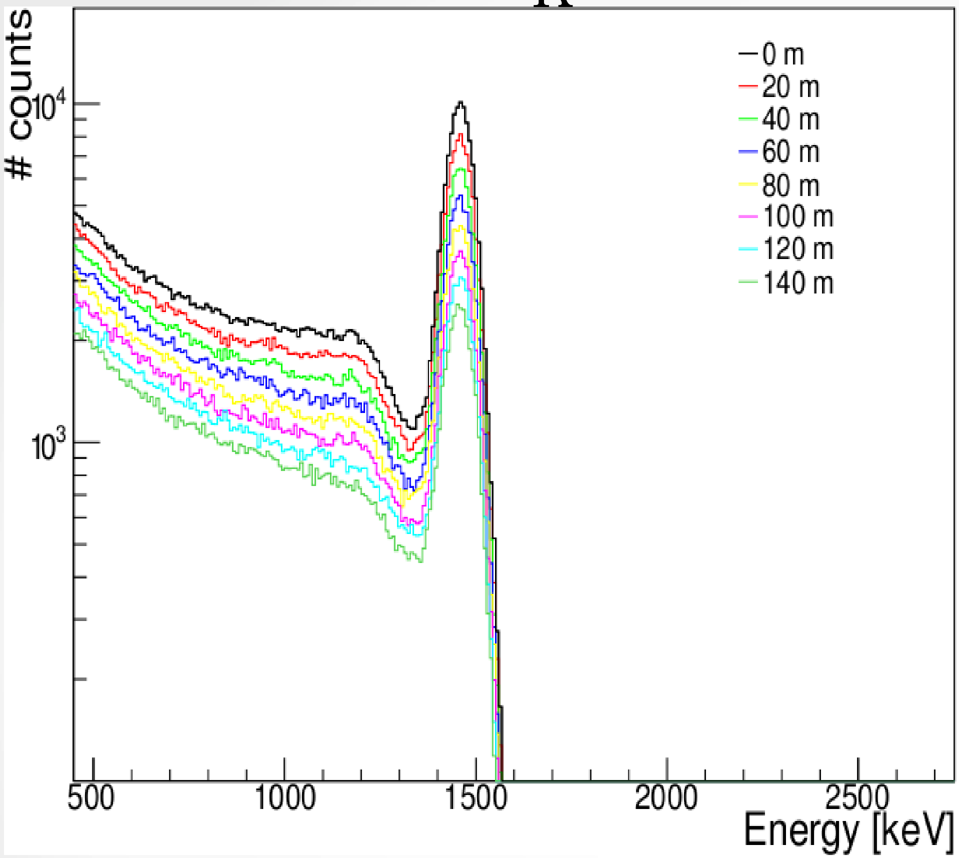

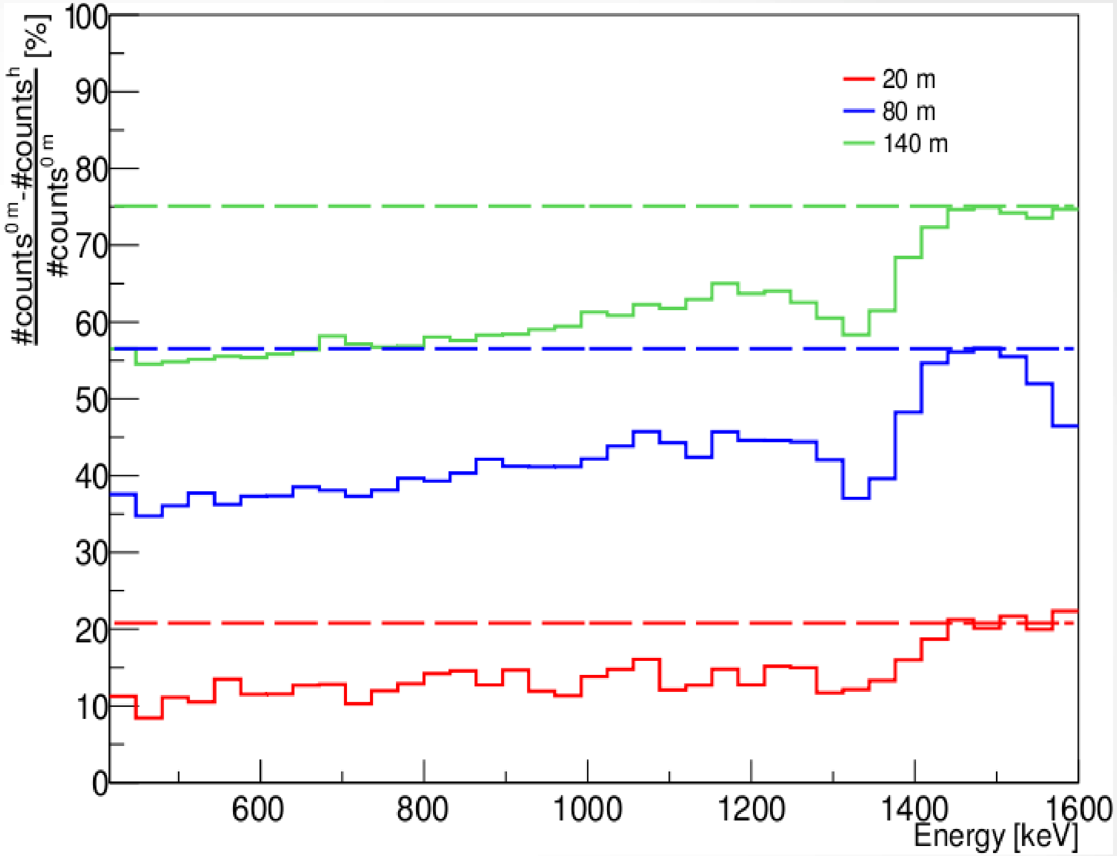

The attenuating effect of air layers of different thickness

is not a simple scaling of the spectra,

but a modification in the spectral shape.

MCFS at different altitudes: U

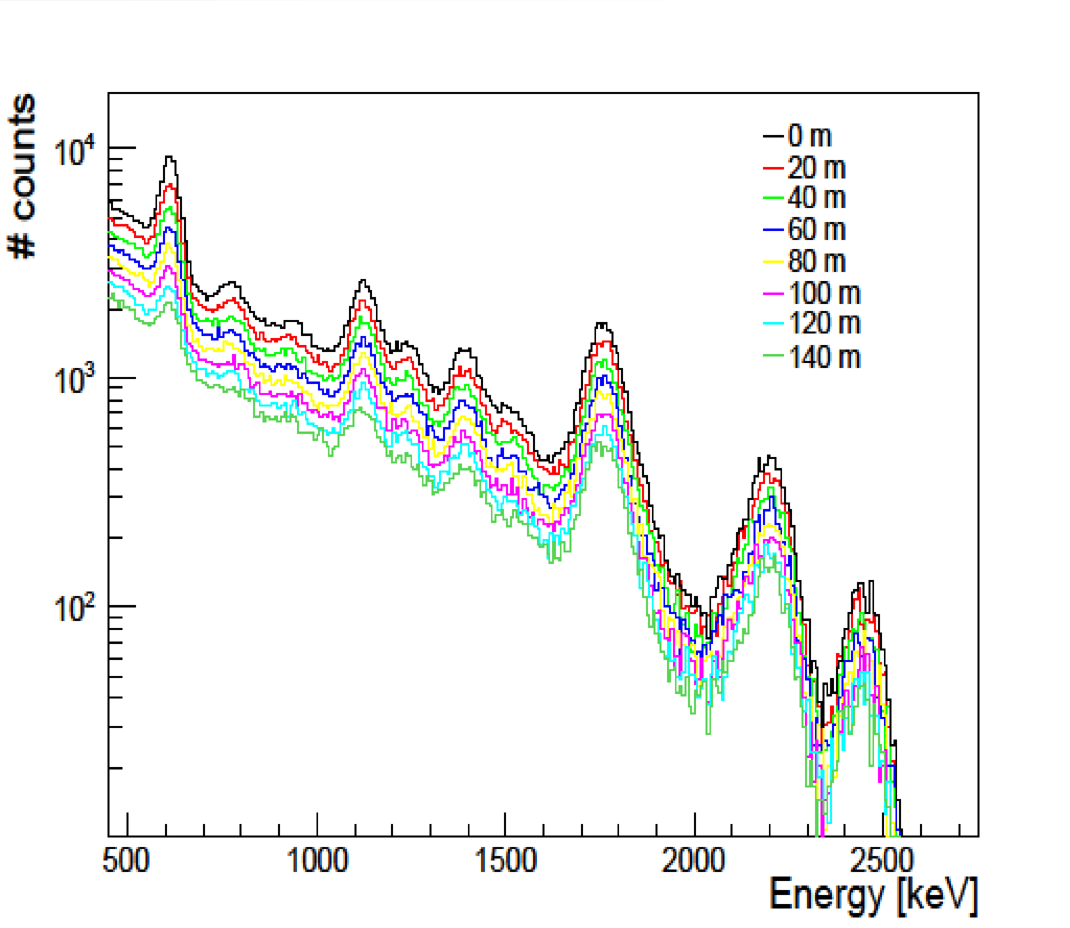

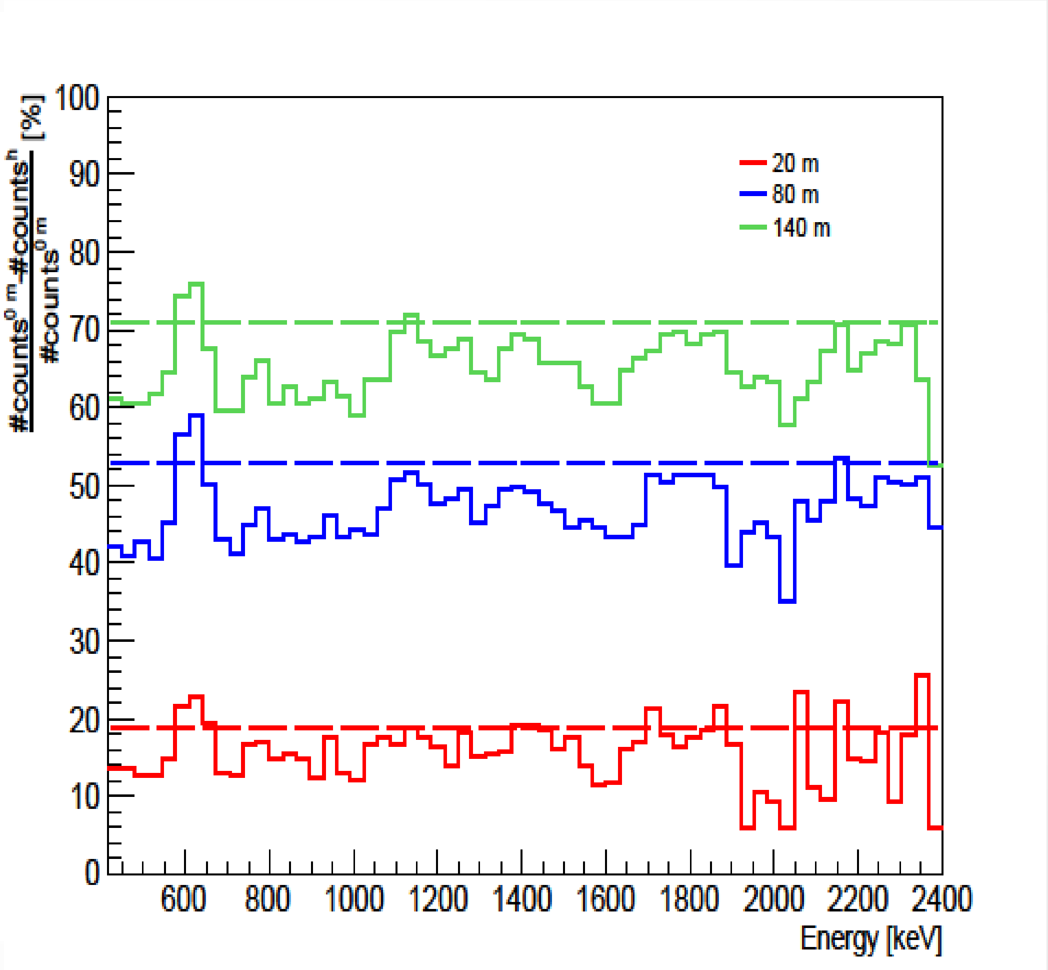

MCFS at different altitudes: Th

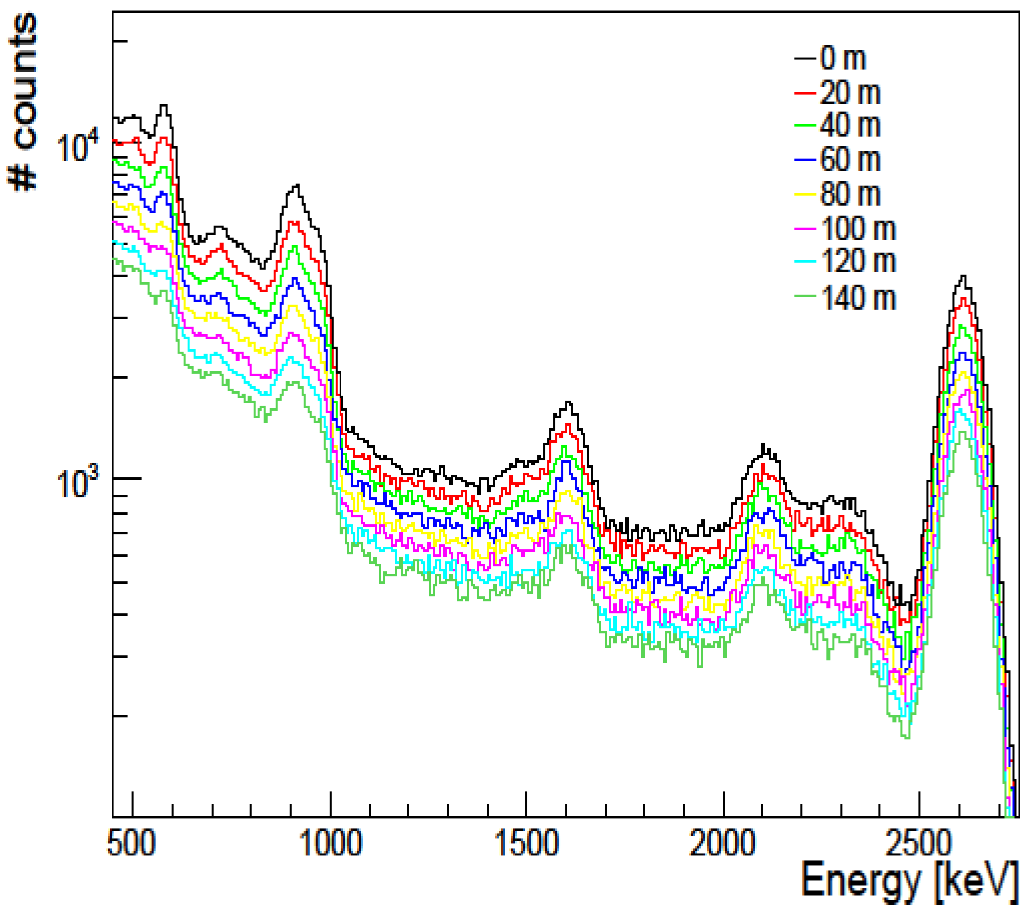

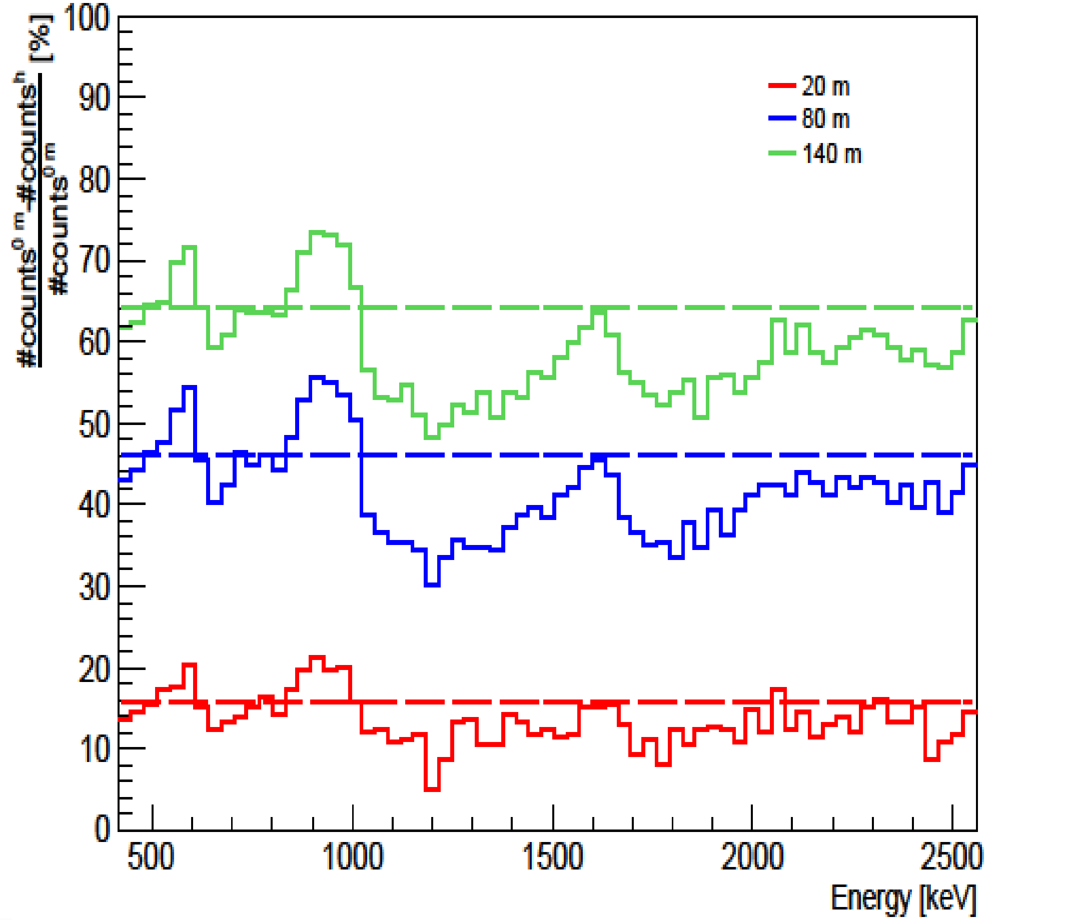

FSA of ground calibration measurements with MCFS

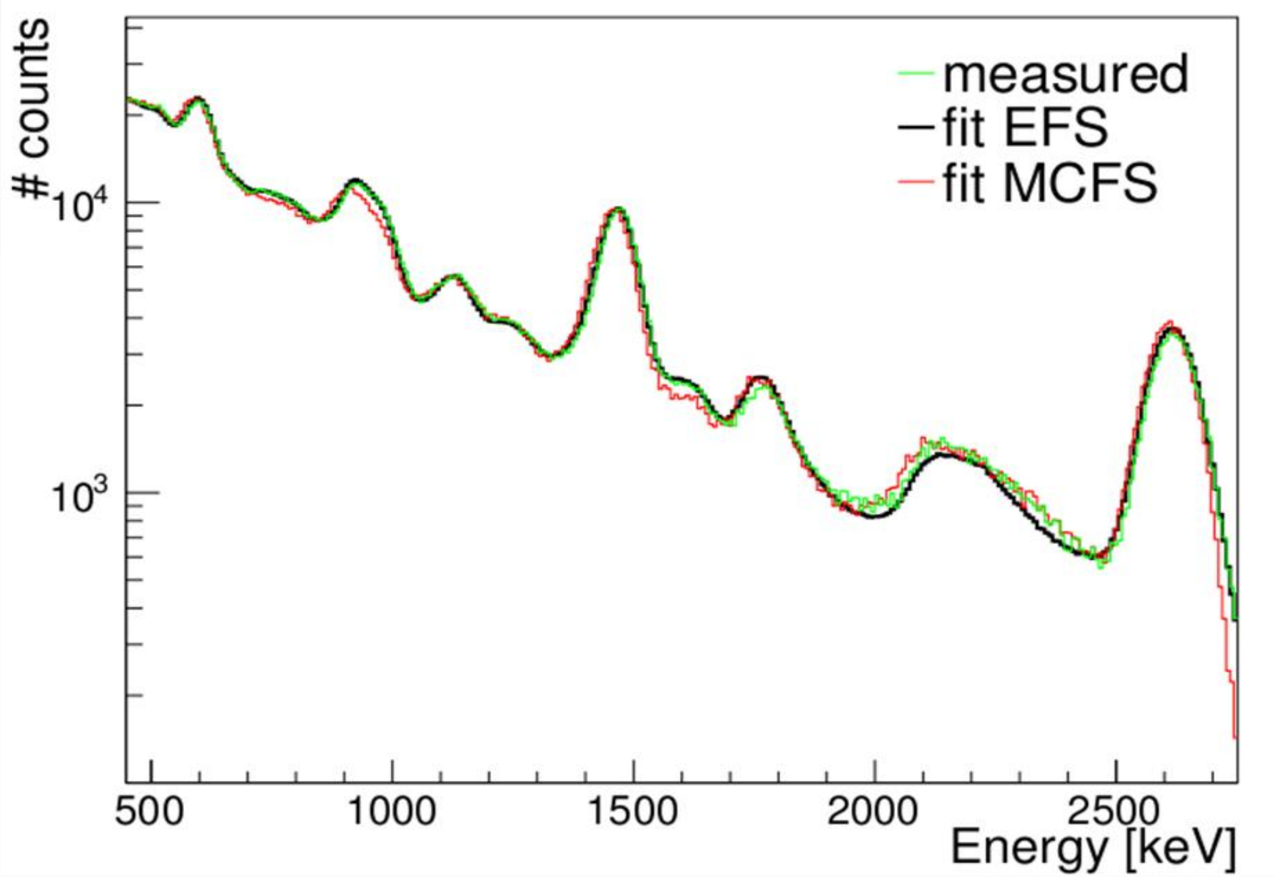

FSA with EFS:
- best agreement between spectral shapes
- overestimated abundances with respect to HPGe

FSA with MCFS:
- good agreement between spectral shapes
- abundances having mean discrepancies with the HPGe values compatible with zero

Histograms of photons areal distributions

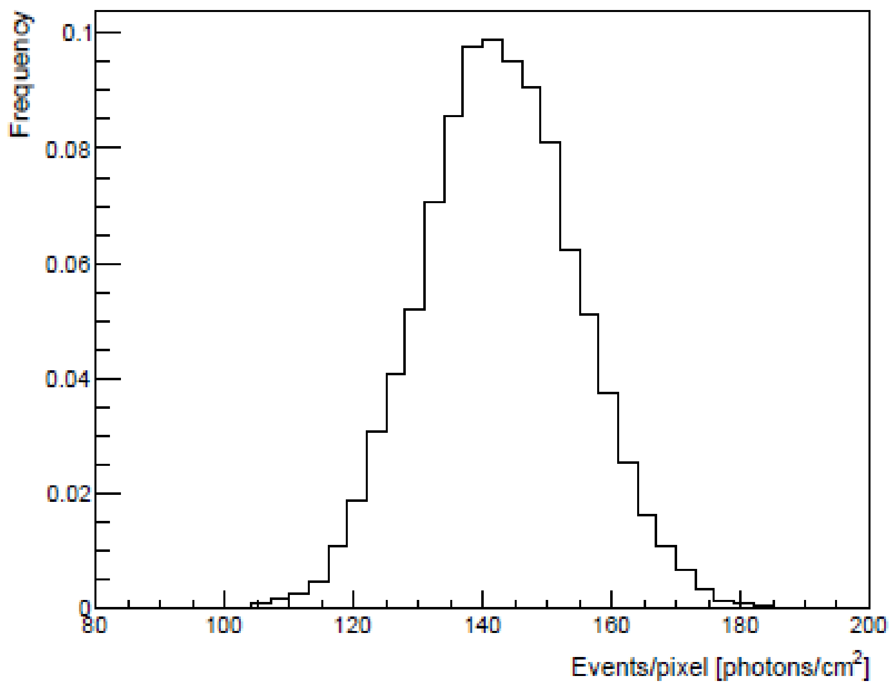

Figure 2.12: distribution of the photons per pixel obtained after the application of the shift procedure to the photons arrival positions on the detection surface. The distribution refers to photons moving upwards and reaching an altitude of 100 m. The histogram binning is 3 photons/cm^2.

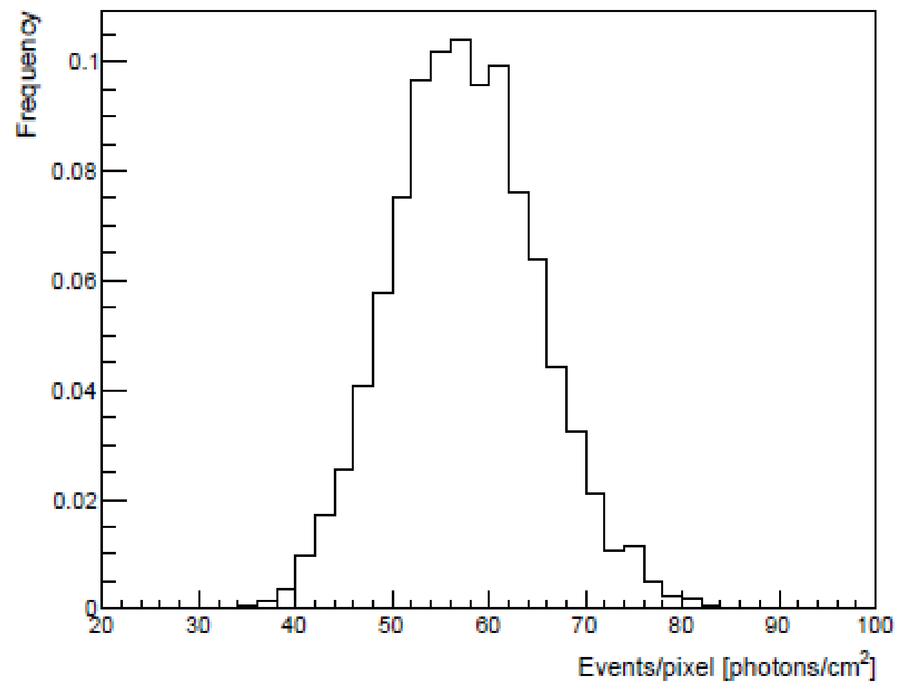

Figure 2.13: distribution of the photons per pixel obtained after the application of the shift procedure to the photons arrival positions on the detection surface. The distribution refers to photons moving downwards and reaching an altitude of 100 m. The histogram binning is 2 photons/cm^2.

^{40}K photopeak flux from a point source for composite air and soil media

Table 3.5: ratios between the theoretical and the Monte Carlo determined values of $\Phi_{circ}(h)$ from a point source buried in a soil volume of thickness equal to 10 cm, 20 cm and 30 cm. The air material is a mixture of 70% nitrogen and 30% oxygen, with a density of 1.3 mg/cm^3. The soil material is a mixture of 70% silicon and 30% magnesium, with a density of 1.5 g/cm^3. The maximum emission polar angle θ^* is equal to 3°.

point source depth	$\Phi^{th}_{circ}/\Phi^{MC}_{circ}$ at 10 m	$\Phi^{th}_{circ}/\Phi^{MC}_{circ}$ at 100 m
10 cm	0.997 ± 0.002	0.995 ± 0.002
20 cm	1.000 ± 0.002	1.000 ± 0.003
30 cm	0.999 ± 0.003	0.998 ± 0.005

$$\Phi_{circ}(h) = \frac{N_h}{\pi R^2} = \frac{S}{\pi(h+t)^2 \tan\theta^{*2}} \frac{\int_0^{\theta^*} \sin\theta \, e^{-\frac{\lambda t + \mu h}{\cos\theta}}}{\int_0^{\theta^*} \sin\theta}$$

S = number oh photons radiated by the point source in the unit time (photons/s);

λ = linear attenuation coefficient of the soil (m^{-1});

t = soil thickness (m);

μ = linear attenuation coefficient of the air (m^{-1}).

Field of view of an ideal gamma-ray detector

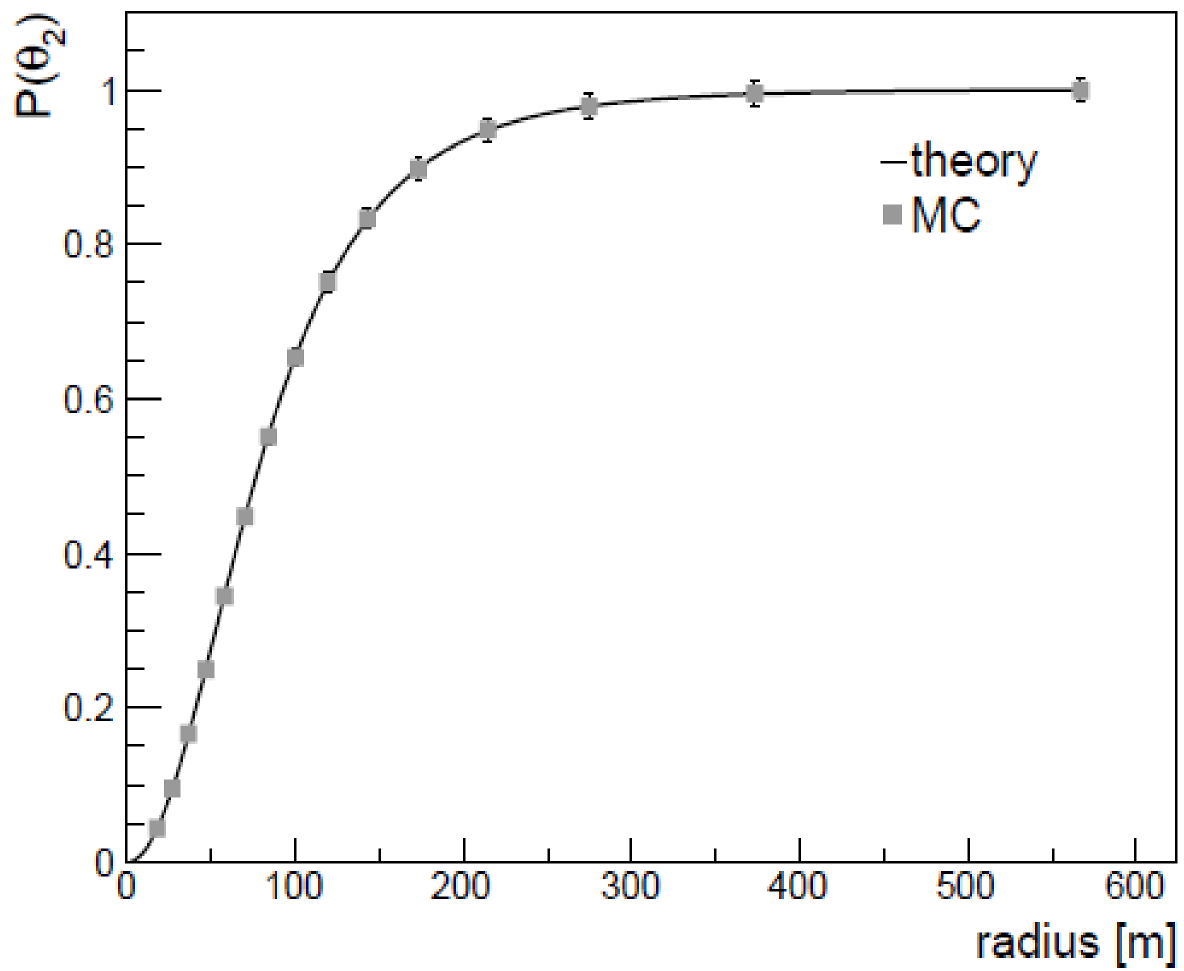

Figure 3.24: Monte Carlo evaluated and theoretical curve of $P(\theta_2)$ for unscattered photons detected at 100 m above the ground level. The diffuse source geometry is a cylinder with infinite radius and infinite thickness.

Field of view of an ideal gamma-ray detector

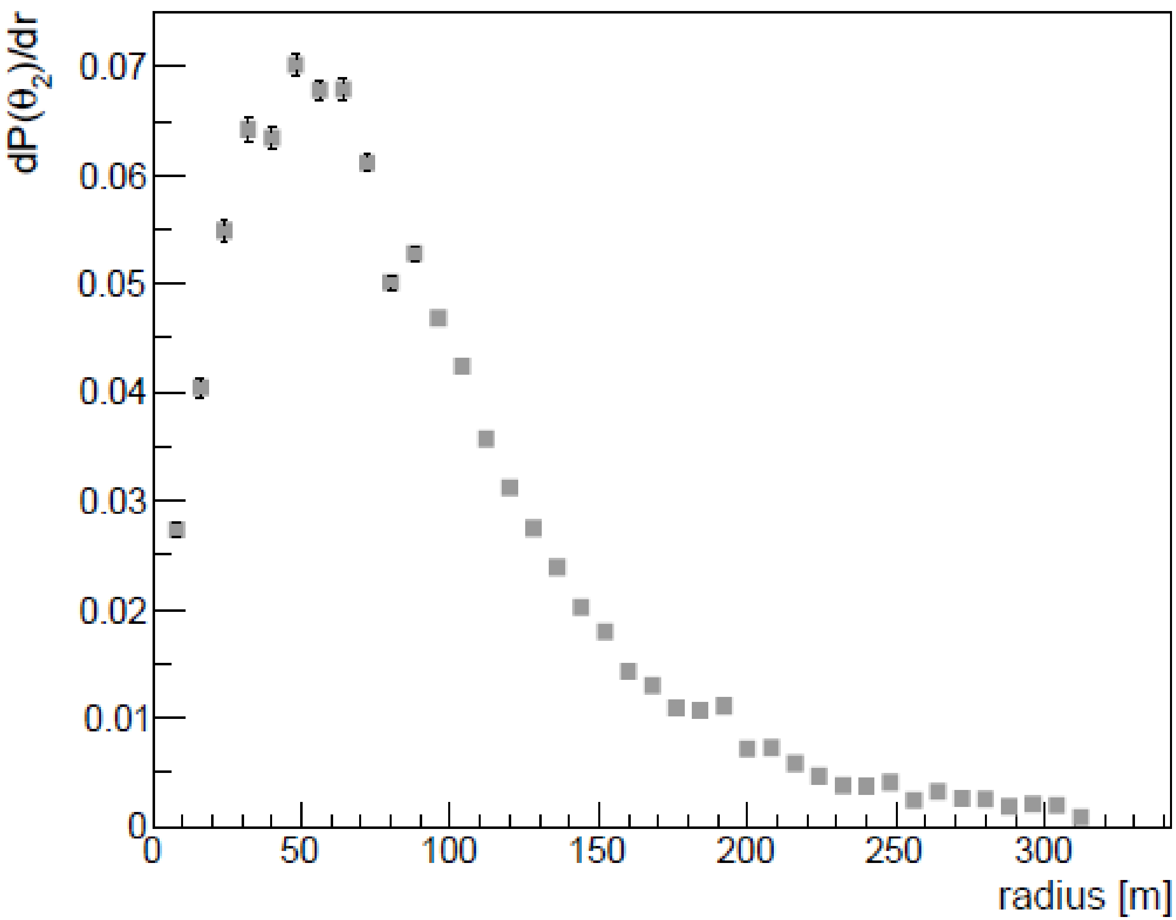

Figure 3.26: Monte Carlo evaluated derivative of $P(\theta_2)$ as function of the radial distance from the center of the detection surface. The source volume geometry is a cylinder with infinite radius and infinite thickness and the detection surface is placed at 100 m above the ground level.

MC_AGRS_16L components

Table 4.2: geometrical dimensions, physical and chemical features of the components of the MC_AGRS_16L model.

MC_AGRS_16L component	Dimensions [mm]	% by weight	Density [g/cm^3]
4L crystal	width = 101.6 height = 101.6 length = 406.4	100 NaI	3.67
Crystal housing	thickness = 1 top plate = 11 bottom plate = 4.75	69 Fe 19 Cr 9 Ni 2 Mn 1 Si	7.93
PMT	radius = 45 length = 146	96 Air 4 Cu	0.34
PVC box	thickness = 10	100 C_2H_3Cl	1.38
1L crystal	width = 102 height = 65 length = 102	100 NaI	3.67
Battery pack	width = 94 height = 65 length = 151	79 Air 21 Pb	2.41

Generated statistics

Radioelement	a [Bq/kg]
^{40}K	1% = 313 Bq/kg
^{238}U	1μg/g = 12.35 Bq/kg
^{232}Th	1μg/g = 4.06 Bq/kg

Radioelement	N [photons/decay]
^{40}K	0.107
^{238}U	2.022
^{232}Th	2.437

$$\gamma_i = n_i c_i t$$

$$n_i = N_i a_i \rho_{soil} V$$

n_i = number of photons radiated per second by the i-th atomic species (photons/sec);

N_i = number of photons emitted per decay by the i-th atomic species (photons/decay);

a_i = specific activity associated to a unitary concentration of the i-th atomic species (Bq/kg);

ρ_{soil} = soil density (kg/m^3);

V = source volume, in every case equal to 1m^3.

c_i = i-th radioelement abundance (% for ^{40}K, μg/g for ^{238}U and ^{232}Th);

t = acquisition time (sec).

Ground based calibration measurements: SR calibration site

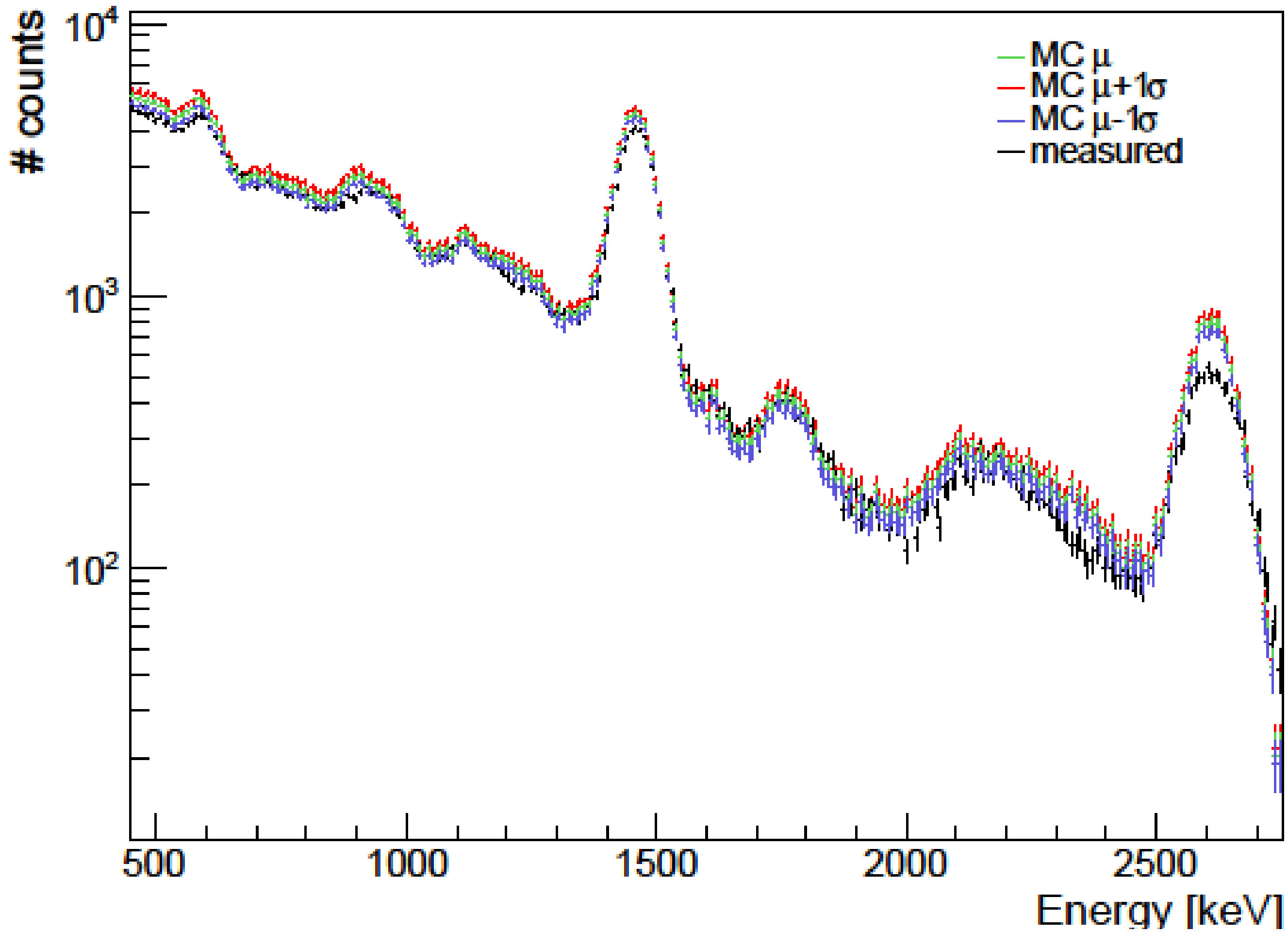

Figure 5.7: in black 5'spectrum (after background subtraction) measured in the SR site and in green the simulated spectrum with soil density equal to 1.6 g/cm^3, soil chemical composition reported in Table 5.3 and radionuclide abundances a(K)= 1.30 %, a(U) = 1.36 μg/g and a(Th) = 7.36 μg/g. The spectra MC $\mu + 1\sigma$ (red) and MC $\mu - 1\sigma$ (blue) are obtained rescaling with $\pm 1\sigma$ abundances for each radioisotope, respectively (cfr. Table 5.1). The measured spectrum and the simulated one with the mean concentration values μ are in agreement with a reduced χ^2=4.5.

Ground based calibration measurements: SM calibration site

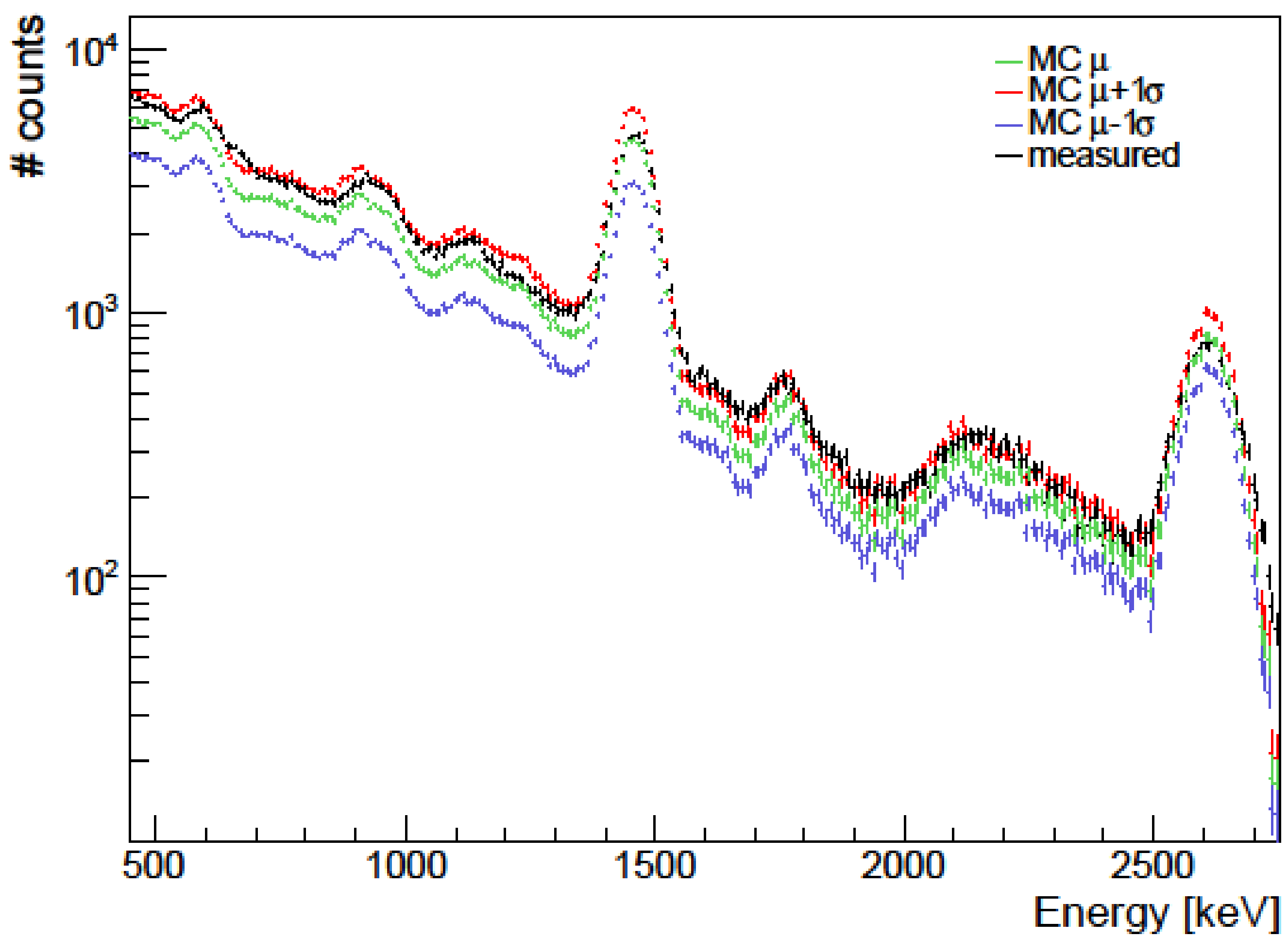

Figure 5.6: in black 5'spectrum (after background subtraction) measured in the SM site and in green the simulated spectrum with soil density equal to 1.6 g/cm^3, soil chemical composition reported in Table 5.4 and radionuclide abundances a(K)= 1.38 %, a(U) = 1.50 μg/g and a(Th) = 7.99 μg/g. The spectra MC $\mu + 1\sigma$ (red) and MC $\mu - 1\sigma$ (blue) are obtained rescaling with $\pm 1\sigma$ abundances for each radioisotope, respectively (cfr. Table 5.1). The measured spectrum and the simulated one with the mean concentration values μ are in agreement with a reduced χ^2=6.6.

K Monte Carlo fundamental spectrum

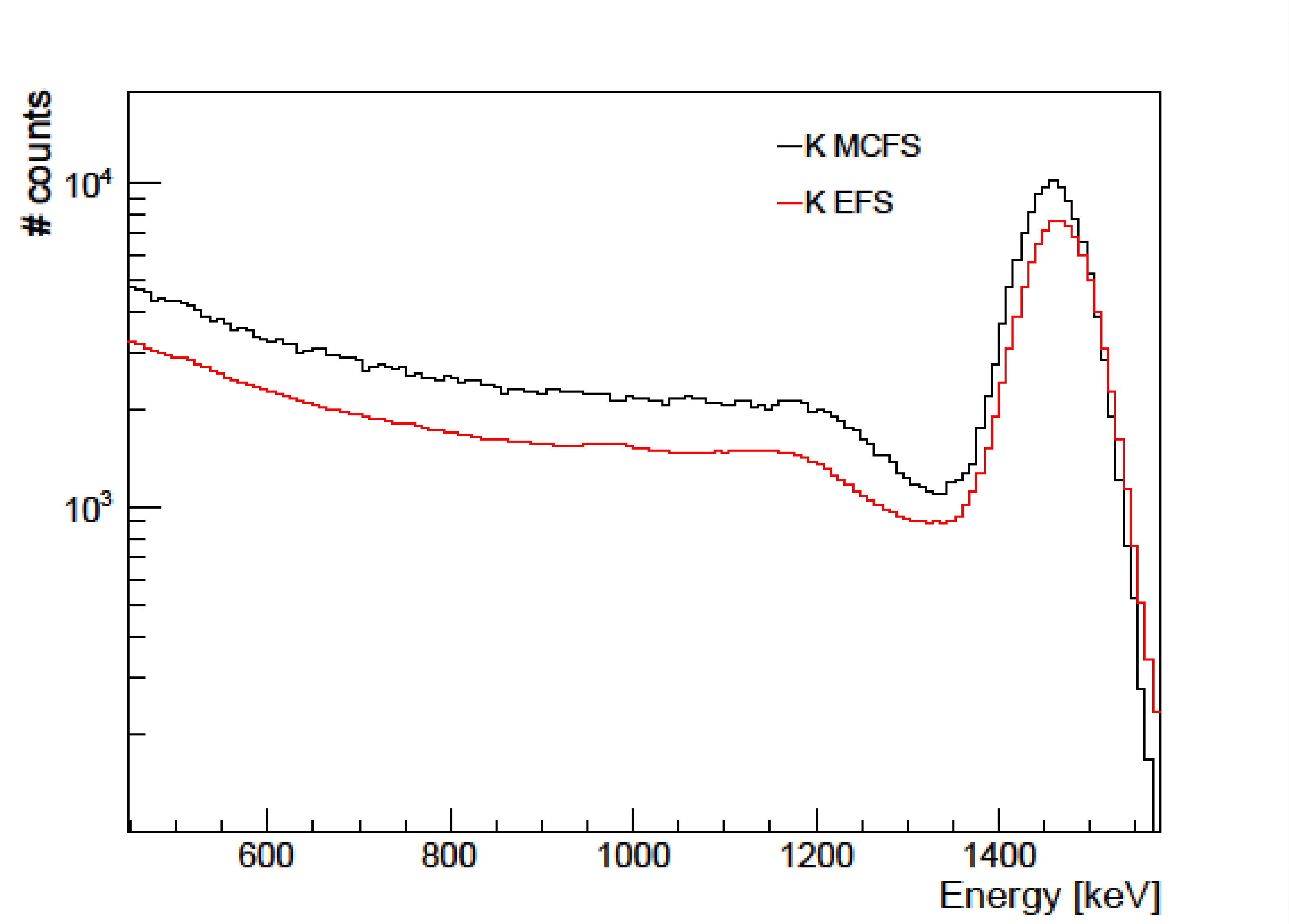

U Monte Carlo Fundamental Spectrum

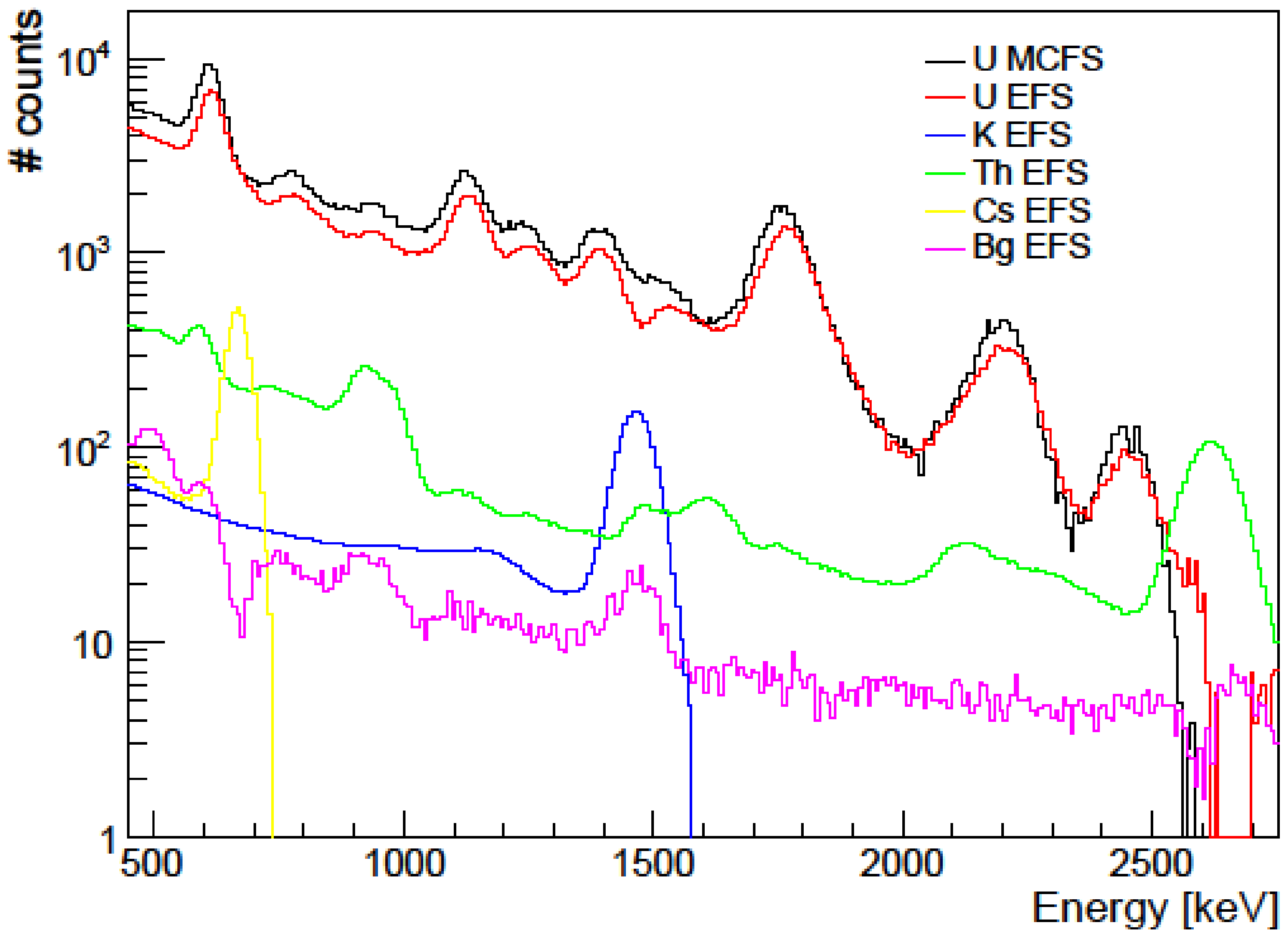

FSA of ground calibration measurements with EFS and MCFS

Table 5.16: potassium, uranium and thorium abundances of the SP, SM and SR calibration sites determined via soil sample measurements with the HPGe detector and via the spectral analysis of the AGRS_16L ground based measurement using both the EFS and the MCFS.

Site	Measurement	K [%]	eU [μg/g]	eTh [μg/g]
SP	HPGe	2.63 ± 0.28	7.45 ± 0.48	36.36 ± 3.28
	EFS	2.87 ± 0.03	8.45 ± 0.16	47.11 ± 0.30
	MCFS	2.35 ± 0.03	9.20 ± 0.17	38.27 ± 0.33
SM	HPGe	1.38 ± 0.44	1.50 ± 0.35	7.99 ± 1.91
	EFS	1.721 ± 0.015	2.15 ± 0.05	10.72 ± 0.10
	MCFS	1.522 ± 0.015	2.25 ± 0.06	9.32 ± 0.11
SR	HPGe	1.30 ± 0.05	1.36 ± 0.11	7.36 ± 0.51
	EFS	1.524 ± 0.013	1.81 ± 0.05	7.42 ± 0.09
	MCFS	1.195 ± 0.012	1.72 ± 0.04	6.07 ± 0.09

Characterization of the site for the airborne dedicated survey

Table 6.1: average natural radionuclide abundances measured in the soil samples collected in the RE site, together with the average abundances determined from in situ measurements. The mean concentration values obtained from the total 100 measurements are also listed.

	K [%]	eU [μg/g]	eTh [μg/g]
HPGe	1.86 ± 0.30	2.65 ± 0.51	9.55 ± 1.40
ZaNaI_10	2.00 ± 0.17	2.06 ± 0.27	9.10 ± 0.62
Average	1.93 ± 0.25	2.35 ± 0.50	9.32 ± 1.09

FSA of airborne survey with MCFS

Analyzed spectrum	K [%]	eU [μg/g]	eTh [μg/g]	χ^2
Average HPGe & ZaNaI_01	1.93 ± 0.25	2.35 ± 0.50	9.32 ± 1.09	/
measured 40 m	2.24 ± 0.04	3.52 ± 0.17	11.03 ± 0.29	1.47
measured 60 m	2.07 ± 0.04	3.90 ± 0.19	9.95 ± 0.30	1.43
measured 80 m	1.99 ± 0.05	4.10 ± 0.20	10.56 ± 0.32	1.36
measured 100 m	1.69 ± 0.05	3.28 ± 0.20	9.37 ± 0.35	1.42
measured 120 m	1.87 ± 0.05	4.44 ± 0.21	9.10 ± 0.34	1.18
measured 140 m	1.78 ± 0.07	5.40 ± 0.28	9.45 ± 0.41	1.50

FSA of airborne survey with MCFS